ANALYSIS OF PP AND PS AMPLITUDE VARIATION WITH OFFSET

A DISSERTATION

Submitted in partial fulfillment of the
requirements for the award of the degree
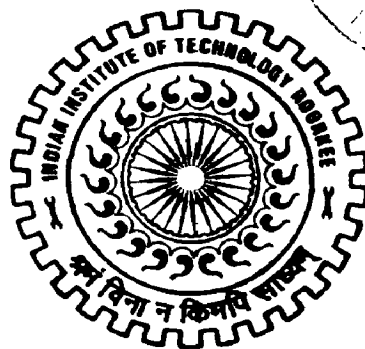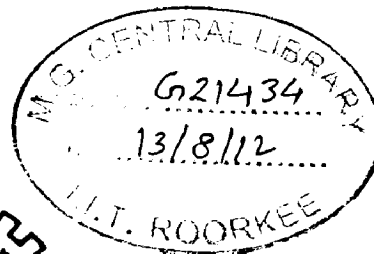*of*

INTEGRATED MASTER OF TECHNOLOGY

in

GEOPHYSICAL TECHNOLOGY

By

URVASHI KESWANI

DEPARTMENT OF EARTH SCIENCES
INDIAN INSTITUTE OF TECHNOLOGY ROORKEE
ROORKEE-247 667 (INDIA)
JUNE, 2012

CANDIDATE'S DECLARATION

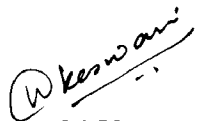I hereby declare that the work, which is being presented in the dissertation entitled, **"ANALYSIS OF PP AND PS AMPLITUDE VARIATION WITH OFFSET"** which is submitted in the partial fulfillments of the requirements for the award of the degree of **Integrated Master of Technology** in **Geophysical Technology**, submitted in the **Department of Earth Sciences, Indian Institute of Technology, Roorkee** is an authentic record of my own work carried under the guidance of **Dr. V. N. Singh**, Professor, Department of Earth Sciences, Indian Institute of Technology, Roorkee.

The matter embodied in the report to the best of my knowledge has not been submitted for the award of degree elsewhere.
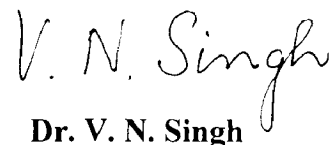
Date: 12-06-2012

Place: Roorkee

Urvashi Keswani

This is to certify that the above statement made by the candidate is correct to the best of my knowledge.

Dr. V. N. Singh

Professor

Department of Earth Sciences

IIT Roorkee

ACKNOWLEDGEMENT

Date: 12-06-2012

Place: Roorkee

Urvashi Keswani,

Integrated M.Tech – 5th yr,

Geophysical Technology,

IIT Roorkee.

ABSTRACT

In the present dissertation an attempt has been made for the analysis of PP and PS amplitude variation with offset for various lithological models relevant to hydrocarbon exploration. Synthetic seismograms have been generated for the models under consideration to study the amplitude variation with offset, both for PP and PS waves. The synthetic seismograms have been generated based on Zoeppritz equations. Following this, inversion of reflection amplitudes in the synthetic seismograms has been carried out to obtain the P wave velocity, S wave velocity and the density. The inversion has been carried out using three methodologies. The first method is based on carrying out a direct inversion, separately for PP and PS waves, using the Aki and Richards' approximations to the Zoeppritz equation. The second method consists of a two term joint inversion method which has been tested. The final method is a three term joint inversion method. The results of the inversions indicate that all the three model parameters, viz., P wave velocity, S wave velocity and the density are inverted satisfactorily by the different inversion methods. Using the PS data set in conjunction with PP data sets can improve the AVO inversion results in some cases.

CONTENTS

3. COMPUTATIONAL ASPECTS

4. RESULTS AND DISCUSSIONS

LIST OF FIGURES

LIST OF TABLES

CHAPTER 1

INTRODUCTION

1.1 Preamble

The exploration for hydrocarbons is being carried out primarily by the seismic reflection technique for a very long time. The continuous sampling, the high resolution of the data and the minimal cost obtainable, make the method an inseparable part of modern oil and gas exploration.

In many cases, seismic reflection profiles are used to locate structures that have the potential to trap hydrocarbons. Anticlines, fault traps, and stratigraphic pinch outs are all easily mapped using seismic reflection data. However, the risk lies in the possibility that the trap may not contain hydrocarbons. Exploration would be more effective if the hydrocarbons could be detected directly on the seismic sections. In the 1960s, geophysicists discovered that the presence of gas often resulted in high-amplitude reflections known as "bright spots" (Ostrander, 1982). The bright spot method was found to have limitations, in that factors other than gas can cause high amplitude reflections. Dry holes drilled into bright spots found igneous intrusions, carbonate or hard streaks, lignites, or wet sands. A test more definitive than bright spots on a stacked section was sought for the direct detection of gas on seismic records, which led to the analysis of amplitude variation with offset on pre-stack data.

The variation of reflection and transmission coefficients with angle of incidence (AVA) (and corresponding increasing offset) is often referred to as offset-dependent reflectivity and is the fundamental basis for amplitude-versus-offset (AVO) analysis. There are two kinds of AVO phenomena according to the types of seismic data. One is P-wave AVO and the other is multi -component AVO corresponding to single component P-wave seismic data and multi - component seismic data, respectively.

At present, AVO analysis is widely used in hydrocarbon detection, lithology identification, and fluid parameter analysis, due to the fact that seismic amplitudes at the boundaries are affected by the variations of the physical properties just above and just below the boundaries. In recent years, a growing number of theories and techniques in seismic data acquisition,

processing, and seismic data interpretation have been developed, updated, and employed. AVO analysis in theory and practice is becoming increasingly attractive.

1.2 P Wave AVO Methods

With the development of multi-offset recordings in the 1960's, lithological estimation methods finally became viable. Early techniques of lithology estimation were focussed on zero-offset or post-stack inversion methods. These methods along with "bright spot" analysis techniques gave a very simple model of the seismic response. Ostrander (1982) demonstrated that gas-sand reflection coefficients vary in an anomalous fashion with increasing offset and showed how to utilize this behaviour as a direct hydrocarbon indicator. Ostrander (1982) further proposed using pre-stack seismic amplitudes to extract information about lithology and pore-fluids. Since then, AVO has been used with varied degrees of success. New developments in seismic acquisition and processing in recent years have improved the promise of this method. Shuey (1985) developed a gradient-intercept method that measures zero-offset reflectivity and changes in Poisson's ratio. This method, though useful, requires a fixed Vp/Vs ratio and thus may be invalid if a poor initial model is used. Smith and Gidlow (1987) developed a method using least-squares inversion to apply a set of model-based weights in an offset dependant manner, to form estimates of fractional Vp and Vs velocities. This method does not assume a fixed background Vp/Vs, but does incorporate a smoothed background model independent of the estimates of fractional compressional and shear velocity, i.e. the difference between the velocities of two layers divided by the average velocity of the same two layers. Fatti et al. (1994) further improved upon the Smith-Gidlow or "Geo-stack" method by incorporating density changes instead of using an empirical relationship between Vp and density (Gardner et al., 1974). This method derives estimates of fractional compressional and shear impedance instead of Vp and Vs directly.

1.3 Converted Wave Seismology

In recent years, the use of P-S seismic data has increased as a result of new developments in acquisition and processing technology. It has been shown that supplementary P-S seismic data increases interpretation confidence, provides additional imaging constraints and is useful to provide rock property estimates. In addition, P-S seismic data can be obtained at relatively

low cost from 3-component (3-C) seismic recordings since conventional sources and receiver geometries are employed.

1.4 Objectives of Dissertation

Following are the objectives of the present dissertation.

a) To perform forward modelling and generate synthetic seismograms for PP and PS amplitude variation with offset (AVO) analysis for various models having different lithologies and fluid content, based on Engelmark (2001). The method of seismic ray tracing is used to generate the ray paths for various models and angles of incidence and Zoeppritz equations are used to compute the reflection coefficients. The forward modelling will help in gaining an understanding of the AVO phenomena for different lithologies and fluid content as evident on the synthetic seismic sections.

b) To invert the reflection amplitudes at different offsets to obtain the P and the S wave velocities and density above and below the reflector surface for a number of lithologies using three different methodologies. The first consist of a direct inversion based on Aki and Richards' approximations (Aki and Richards, 2002). The other two are based on a joint inversion methodology proposed by Stewart (1990). This study will indicate the efficiency of each inversion scheme for yielding physical properties of the subsurface.

1.5 Plan of the Thesis

In chapter 2, a theoretical background of the Zoeppritz equations are presented. This involves solution of a boundary value problem when a seismic ray is incident at the surface separating two semi infinite solid elastic media. The solution of this problem gives expressions for reflection coefficient as a function of medium properties and angle of incidence. The Aki and Richards (2002) approximations to the Zoeppritz equation have also been presented along with an outline of the theory for inverting the synthetic data using the three inversion methodologies under consideration in this thesis. The first is based on a direct inversion using the Aki Richards approximations and the other two are based on a joint inversion methodology by Stewart (1990).

In chapter 3, the computational aspects of the generation of synthetic seismograms and of the inversion methodologies are presented.

In chapter 4, the synthetic seismograms have been discussed for each model under consideration and the results of the inversion using the three methods are evaluated.

In chapter 5, conclusions arrived at as a result of this study have been presented.

CHAPTER 2

THEORETICAL ASPECTS

2.1 Principles of AVO

When seismic waves travel in the earth and encounter lithological boundaries with velocity and density contrasts, the energy of the incident wave is partitioned at each boundary. For a source of compressional wave energy, there is a reflected and a transmitted wave of the same type. In addition part of the incident energy is also converted to that of shear waves resulting in reflected and transmitted waves of S type. Thus an incident wave of P-type gives rise to four new waves, two reflected waves of P type and S type and two transmitted waves of P type and S type. The shear (S) waves so generated are known as mode converted S – waves. When the incident wave is normally incident at the boundary, no mode conversion takes place. Such mode conversions are predicted theoretically and are actually recorded when field experiments are carried out.

The fraction of the incident energy that is reflected depends upon the angle of incidence. Analysis of reflection amplitudes as a function of incidence angle can sometime be used to detect lateral changes in elastic properties of reservoir rocks, such as the change in Poisson's ratio. This may then suggest a change in the ratio of P wave velocity to S wave velocity, which in turn may imply a change in fluid saturation within the reservoir rocks.

Starting with the equations of motion and Hooke's law, one can derive and solve the wave equations for plane elastic waves in isotropic media. Then, using the equations of continuity for the vertical and tangential components of stress and strain at a layer boundary, plane wave solutions and Snell's law that relates propagation angles to wave velocities, one obtains the equation for computing the amplitudes of the reflected and transmitted P- and S- wave.

In this chapter the solution to the problem of P wave reflection to P and as mode converted S - waves in the presence of two homogeneous semi infinite media has been presented. The method described below has been adapted from Aki and Richards (2002). Only plane waves have been taken into consideration.

5

A layered half space consisting of perfectly elastic, homogeneous and isotropic media has been assumed. The interfaces are assumed to be horizontal and infinite in horizontal extent. In each layer following equation of motion is satisfied.

$$\rho \mathbf{u} = (\lambda + 2\mu)\,grad\ div\,\mathbf{u} - \mu\,curl\,curl\,\mathbf{u} \qquad (2.1)$$

where $\mathbf{u}$ is the displacement vector, with components u, v, w in the x, y and z directions respectively, ρ the density and λ, μ are Lame's parameters. Body forces as well as terms describing seismic sources have been neglected.

To solve equation (2.1) use is made of the displacement potentials. A Cartesian coordinate system is chosen with z axis pointing positive downward into the lower space. The surface separating the two half spaces coincides with the plane z = 0. All wave motion is assumed to be confined to the vertical plane so that all quantities (displacement and stresses) become independent of the y-coordinate.

The displacement vector $\mathbf{u}$ can be expressed in terms of a scalar potential φ and a vector potential $\mathbf{\psi}$

$$\mathbf{u} = grad\,\varphi + curl\,\mathbf{\psi} \qquad (2.2)$$

When all the quantities are independent of the y co-ordinates, equation (2.2) can be written as

$$u = \partial\varphi / \partial x - \partial\psi / \partial y$$
$$w = \partial\varphi / \partial x + \partial\psi / \partial y \qquad (2.3)$$

where ψ is the y component of $\mathbf{\psi}$.

Using the expression (2.3) in the equation (2.1), wave equation in terms of φ and ψ is:

$$\nabla^2 \varphi = (1 / \alpha^2)\,\partial^2 \varphi / \partial t^2$$
$$\nabla^2 \psi = (1 / \beta^2)\,\partial^2 \psi / \partial t^2 \qquad (2.4)$$

6

Here, $\nabla^2 = \partial^2/\partial x^2 + \partial^2/\partial z^2$ is the Laplacian operator in two dimensions. Equation (2.4) involving φ and ψ stands for P and SV wave propagation. $\alpha = [(\lambda + 2\mu)/\rho]^{1/2}$ is the P wave velocity and $\beta = [\mu/\rho]^{1/2}$ is the S wave velocity.

The wave propagation in the presence of two elastic solid half spaces has to satisfy the boundary conditions at the interface. The boundary conditions require continuity of displacements and stresses.

If Cartesian coordinates are used for P- SV propagation, the normal and the tangential traction components are:

$$P_{zx} = \mu\left(\frac{\partial u}{\partial z} + \frac{\partial w}{\partial x}\right) = 2\mu\frac{\partial^2\phi}{\partial z\partial x} \qquad (2.5)$$

$$P_{zz} = \lambda\left(\frac{\partial u}{\partial x} + \frac{\partial w}{\partial z}\right) + 2\mu\left(\frac{\partial u}{\partial z}\right) = \lambda\nabla^2\phi + 2\mu\frac{\partial^2\phi}{\partial z^2} \qquad (2.6)$$

The stresses and displacements are continuous at the interface $z = 0$

2.2 Reflection - Transmission coefficients

Let a monochromatic simple harmonic P wave be incident on the interface between two homogeneous elastic half spaces at an angle of incidence i_1. At the interface this wave suffers reflection and transmission, giving rise to two reflected and transmitted waves (Figure 2.1).
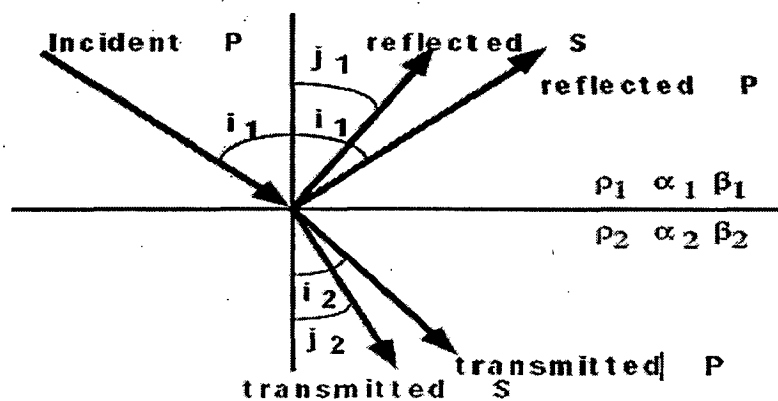
Figure 2.1: Plane P wave incident from the first medium; waves undergo reflection and transmission at the boundary. (Aki and Richards, 2002)

Let the amplitude of the down going incident P wave within the first medium be denoted by P_1^d. The four waves after reflection and transmission have displacement amplitudes P_1^u, S_1^u, P_2^d, S_2^d. Subscripts are used to distinguish the medium in which the wave is propagating and superscript indicates direction of propagation of wave (d for downward and u for upward).

Displacements for incident and scattered waves are given as:

Down going incident P wave in medium 1:

$$P_1^d(\sin i_1, 0, \cos i_1)\exp[i\omega\{px + (\cos i_1 / \alpha_1)z - t\}] \qquad (2.7)$$

Up going reflected P wave in medium 1:

$$P_1^u(\sin i_1, 0, -\cos i_1)\exp[i\omega\{px - (\cos i_1 / \alpha_1)z - t\}] \qquad (2.8)$$

Up going reflected SV wave in medium 1:

$$S_1^u(\cos j_1, 0, \sin j_1)\exp[i\omega\{px - (\cos i_1 / \beta_1)z - t\}] \qquad (2.9)$$

Down going transmitted P wave in medium 2:

$$P_2^d(\sin i_2, 0, \cos i_2)\exp[i\omega\{px + (\cos i_2 / \alpha_2)z - t\}] \qquad (2.10)$$

Down going transmitted SV wave in medium 2:

$$S_2^d(\cos j_2, 0, -\sin j_2)\exp[i\omega\{px + (\cos i_2 / \beta_2)z - t\}] \qquad (2.11)$$

In the above equations (2.7 to 2.11), p is the ray parameter $(= (\sin i_1) / \alpha_1)$, i_1, i_2 are the angles that reflected P and transmitted P – wave make with the normal to the interface, j_1, j_2 are the angles that the reflected S- wave and transmitted S – wave make with the normal to the interface, and ω is the angular frequency of the wave.

Also,

$$p = \frac{\sin i_1}{\alpha_1} = \frac{\sin i_2}{\alpha_2} = \frac{\sin j_1}{\beta_1} = \frac{\sin j_2}{\beta_2}$$

The ray parameter p remains unchanged for all reflected and transmitted waves. This arises when continuity of horizontal displacements u_1 and u_2 is applied at the interface $z = 0$.

At the boundary $z = 0$, from continuity of displacements u, w and the stresses P_{zx}, P_{zz}, we obtain the following four equations.

$$\left(P_1^d + P_1^u\right)\sin i_1 + S_1^u \cos j_1 = P_2^d \sin i_2 + S_2^d \cos j_2 \tag{2.12}$$

$$\left(P_1^d - P_1^u\right)\cos i_1 + S_1^u \sin j_1 = P_2^d \cos i_2 - S_2^d \sin j_2 \tag{2.13}$$

and

$$2\rho_1\beta_1 p \cos i_1 \left(P_1^d + P_1^u\right) - S_1^u \rho_1\beta_1 \left(1 - 2\beta_1^2 p^2\right)$$
$$= 2\rho_2\beta_2^2 p \cos i_2 P_2^d + S_2^d \rho_2\beta_2 \left(1 - 2\beta_2^2 p^2\right) \tag{2.14}$$

$$\rho_1\alpha_1\left(1 - 2\beta_1^2 p^2\right)\left(P_1^d + P_1^u\right) - 2\rho_1\beta_1^2 p \cos j_1 S_1^u$$
$$= \rho_2\alpha_2\left(1 - 2\beta_2^2 p^2\right)P_2^d - 2\rho_2\beta_2^2 p \cos j_2 S_2^d \tag{2.15}$$

Rearranging these equations so that scattered waves are all on the left side and incident waves on the right side, equations can be written as:

$$M\begin{pmatrix} P_1^u \\ S_1^u \\ P_2^d \\ S_2^d \end{pmatrix} = N\begin{pmatrix} P_1^d \\ 0 \\ 0 \\ 0 \end{pmatrix} \tag{2.16}$$

Where M and N are coefficient matrices given as:

$$M = \begin{pmatrix} -\alpha_1 p & \cos j_1 & \alpha_2 p & \cos j_2 \\ \cos i_1 & -\beta_1 p & \cos i_2 & -\beta_2 p \\ 2\rho_1\beta_1^2 p \cos i_1 & \rho_1\beta_1(1-2\beta_1^2 p^2) & 2\rho_2\beta_2^2 p \cos i_2 & \rho_2\beta_2(1-2\beta_2^2 p^2) \\ -\rho_1\alpha_1(1-2\beta_1^2 p^2) & 2\rho_1\beta_1^2 p^2 \cos j_1 & \rho_2\alpha_2(1-2\beta_2^2 p^2) & -2\rho_2\beta_2^2 p \cos j_2 \end{pmatrix}$$

(2.17)

$$N = \begin{pmatrix} \alpha_1\rho \\ \cos i_1 \\ 2\rho_1\beta_1^2 p \cos i_1 \\ \rho_1\alpha_1(1-2\beta_1^2 p^2) \end{pmatrix}$$

(2.18)

In case the downgoing P wave in the first medium has unit amplitude, the amplitude of the reflected and transmitted waves is identical with the reflection and transmission coefficients for displacement.

2.3 Explicit Expressions for Reflection and Transmission Coefficients

In the present work, the coefficients of interest are those associated with reflected P and reflected S waves and the transmitted P and the transmitted S waves when a P wave is incident from above. Consequently, these reflection coefficients are defined as given below:

P wave reflection coefficient R_{pp}

S wave reflection coefficient R_{ps}

P wave transmission coefficient T_{pp}

S wave transmission coefficient T_{ps}

The matrix $M^{-1}N$ (obtained from equation 2.16) by putting P_1^d equal to unity, gives

$[R_{pp}, R_{ps}, T_{pp}, T_{ps}]^T$, i.e.,

$$
\begin{bmatrix} R_{pp} \\ R_{ps} \\ T_{pp} \\ T_{ps} \end{bmatrix}^{T} = M^{-1}N \tag{2.19}
$$

The explicit expressions for R_{pp}, R_{ps}, T_{pp}, T_{ps} are given below (after Aki and Richards, 2002)

$$
R_{pp} = \left[\left(b \frac{\cos i_1}{\alpha_1} - c \frac{\cos i_2}{\alpha_2} \right) F - \left(a + d \frac{\cos i_1}{\alpha_1} \frac{\cos j_2}{\beta_2} \right) H \rho^2 \right] / D \tag{2.20}
$$

$$
R_{ps} = -2 \frac{\cos i_1}{\alpha_1} \left(ab + cd \frac{\cos i_2}{\alpha_2} \frac{\cos j_2}{\beta_2} \right) \frac{p \alpha_1}{\beta_1 D} \tag{2.21}
$$

$$
T_{pp}^{d} = 2 \rho_1 \frac{\cos i_1}{\alpha_1} F \frac{\alpha_1}{\alpha_2 D} \tag{2.22}
$$

$$
T_{pp}^{u} = 2 \rho_2 \frac{\cos i_2}{\alpha_2} F \frac{\alpha_2}{\alpha_1 D} \tag{2.23}
$$

$$
T_{ps}^{d} = 2 \rho_1 \frac{\cos j_1}{\beta_1} E \frac{\beta_1}{\beta_2 D} \tag{2.24}
$$

$$
T_{ps}^{u} = 2 \rho_2 \frac{\cos j_2}{\beta_2} E \frac{\beta_2}{\beta_1 D} \tag{2.25}
$$

where,

$$
a = \rho_2 \left(1 - 2\beta_2^2 p^2 \right) - \rho_1 \left(1 - 2\beta_1^2 p^2 \right)
$$

$$
b = \rho_2 \left(1 - 2\beta_2^2 p^2 \right) - 2\rho_1 \left(\beta_1^2 p^2 \right)
$$

$$
c = \rho_1 \left(1 - 2\beta_1^2 p^2 \right) - 2\rho_2 \left(\beta_2^2 p^2 \right)
$$

$$
d = 2 \left(\rho_2 \beta_2^2 - \beta_1^2 \rho_1 \right)
$$

$$F = b\frac{\cos j_1}{\beta_1} + c\frac{\cos j_2}{\beta_2}$$

$$F = a - d\frac{\cos i_2}{\alpha_2}\frac{\cos j_1}{\beta_1}$$

$$D = \frac{\det M}{\alpha_1 \alpha_2 \beta_1 \beta_2} \qquad (2.26)$$

The above expressions are the Zoeppritz equations for reflection and transmission coefficients.

2.4 Aki Richards Approximation to Zoeppritz equations

Explicit expressions for reflection and transmission coefficients for incident P and S- waves have been given in Aki and Richards (2002). These equations are quite complicated and non linear, and do not provide a simple way of understanding as to how the physical properties on either side of the interface influence the reflection and transmission coefficients. Aki and Richards (2002) provide approximate expression for some special cases.

If the contrast between the two half spaces under consideration is small, transmission coefficients will be large for waves that retain the same mode of propagation, but all other scattering coefficients will be small. Thus if the change in the properties denoted by $\Delta\rho = \rho_2 - \rho_1$ for density, $\Delta\alpha = \alpha_2 - \alpha_1$ for P –wave velocity and $\Delta\beta = \beta_2 - \beta_1$ for S wave velocity and the ratios $\Delta\rho/\rho, \Delta\alpha/\alpha$ and $\Delta\beta/\beta$ have magnitudes much less then unity (where ρ, α, β are the mean values of density and velocities), equations (2.20) and (2.21) can be written as,

$$R_{pp}(\theta) \sim \frac{1}{2}\left(1 - 4\frac{\beta^2}{\alpha^2}\sin^2\theta\right)\frac{\Delta\rho}{\rho} + \frac{1}{2\cos^2\theta}\frac{\Delta\alpha}{\alpha} - \frac{4\beta^2}{\alpha^2}\sin^2\theta\frac{\Delta\beta}{\beta} \qquad (2.27)$$

$$R_{ps}(\theta) \sim \frac{-\alpha\tan\varphi}{2\beta}\left[\left(1 - 2\frac{\beta^2}{\alpha^2}\sin^2\theta + 2\frac{\beta}{\alpha}\cos\theta\cos\varphi\right)\frac{\Delta\rho}{\rho} - \left(4\frac{\beta^2}{\alpha^2}\sin^2\theta - 4\frac{\beta}{\alpha}\cos\theta\cos\varphi\right)\frac{\Delta\beta}{\beta}\right]$$

$$(2.28)$$

In the equations (2.27) and (2.28),

$$\Delta \rho = \rho_2 - \rho_1, \ \rho = (\rho_1 + \rho_2)/2 \quad\quad (2.29)$$

$$\Delta \alpha = \alpha_2 - \alpha_1, \ \alpha = (\alpha_1 + \alpha_2)/2 \quad\quad (2.30)$$

$$\Delta \beta = \beta_2 - \beta_1, \ \beta = (\beta_1 + \beta_2)/2 \quad\quad (2.31)$$

$$\theta = (i_1 + i_2)/2, \ \varphi = (j_1 + j_2)/2 \quad\quad (2.32)$$

In the present study, the Zoeppritz equations (2.16) have been used to generate the reflection and transmission coefficients for the synthetic seismogram, whereas the Aki Richards approximations (2.27) and (2.28) are used for inverting the reflection coefficients corresponding to the first reflector in the synthetic seismograms to obtain values of $\Delta \rho / \rho, \Delta \alpha / \alpha$ and $\Delta \beta / \beta$.

2.5 Synthetic Seismogram

Consider a three layered earth model. The ray paths of PP wave reflections and PS wave reflections are shown as follows:
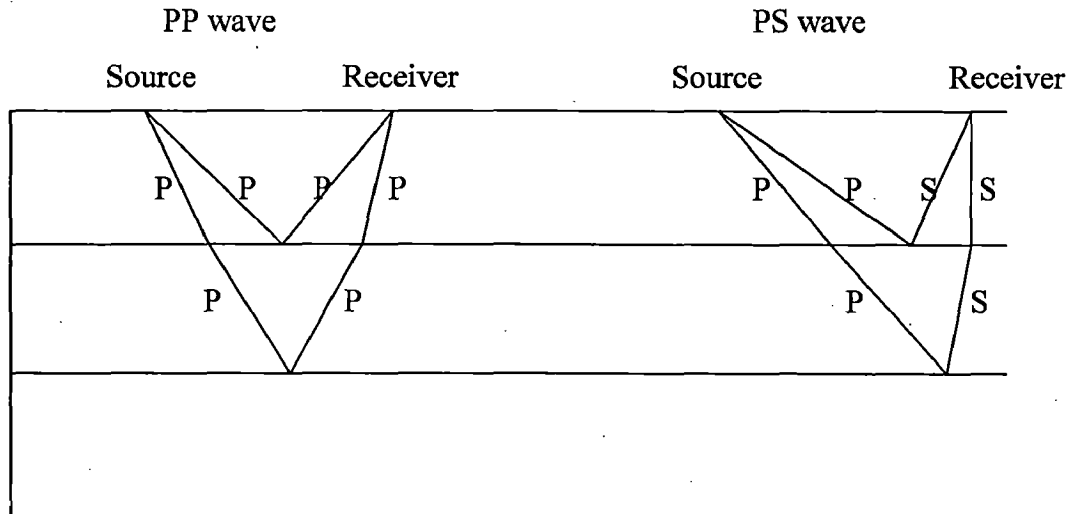

Figure 2.2: Synthetic PP and PS seismogram ray paths for a single source – receiver pair.

Each ray starts at a particular take off angle from the source S, gets reflected and refracted at various interfaces and finally returns to the surface to be detected and recorded. The

13

expression for the vertical component U_z and the radial component U_r of displacement for PP reflected waves and PS reflected waves respectively at the free surface of the Earth model is given by, after modifications of the expressions given by Aki and Richards (2002).

$$U_z(0,t) = \left\{ \frac{-2\frac{\alpha}{\beta^2}\frac{\cos i}{\alpha}\left(\frac{1}{\beta^2}-2p^2\right)}{\left(\frac{1}{\beta^2}-2p^2\right)^2 + 4p^2\frac{\cos i}{\alpha}\frac{\cos j}{\beta}} \right\} \times \text{Product} \times R_{pp} \times \exp(t - \text{Sum}) \qquad (2.33)$$

$$U_r(0,t) = \left\{ \frac{4\frac{p}{\beta}\frac{\cos i}{\alpha}\frac{\cos j}{\beta}}{\left(\frac{1}{\beta^2}-2p^2\right)^2 + 4p^2\frac{\cos i}{\alpha}\frac{\cos j}{\beta}} \right\} \times \text{Product} \times R_{ps} \times \exp(t - \text{Sum}) \qquad (2.34)$$

where, product represents the product of transmission coefficients of downward travelling waves and transmission coefficient of upward travelling waves for PP waves or PS waves respectively.

Consider the situation in the Figure 2.3, where a P - wave source and a receiver are both buried below the free surface in a half space. At the receiver, three waves are received – a direct P wave, a reflected P wave and a reflected S wave. These are separated by short time intervals. As the receiver is moved close to the free surface, the pulses representing the three pulses coalesce into one large pulse. This effect of free surface depends on the angle at which the ray path is incident at the free surface. A similar situation exists when an S wave emanates from the surface.

Figure 2.3: Free surface effect.

The first terms (on the right hand side) in equations (2.33) and (2.34) represents the free surface effect on amplitude of up going (reflected) P and S waves. In these terms, i and j are the angles that P and S waves make with the normal at the free surface and α, β are the velocities below the free surface.

Sum is the travel time of the reflected PP or PS wave respectively.

2.6 Inversion based on Aki and Richards (2002) Approximations

For the inversion of the reflection coefficients, a situation has been visualized, when , after a seismic reflection, common midpoint (CMP) gathers are obtained where all the traces corresponding to a common depth point or common conversion point are put in one group. For such traces, the shot receiver distances or the offsets vary giving range of angles of incidence. In this way, a number of equations say, n (corresponding to the number of offsets) ,of the type (2.27) and (2.28) are obtained, one equation of each type for every angle of incidence. Equations (2.27) and (2.28) can then be rewritten as

$$R_{pp}(\theta) \sim A_p \frac{\Delta\rho}{\rho} + B_p \frac{\Delta\alpha}{\alpha} + C_p \frac{\Delta\beta}{\beta}$$

$$R_{ps}(\theta) \sim A_s \frac{\Delta\rho}{\rho} + B_s \frac{\Delta\beta}{\beta} \qquad (2.35)$$

Where,

$$A_p = \frac{1}{2}\left(1 - 4\frac{\beta^2}{\alpha^2}\sin^2\theta\right)$$

$$B_p = \frac{1}{2\cos^2\theta}$$

$$C_p = -\frac{4\beta^2}{\alpha^2}\sin^2\theta$$

$$A_s = \frac{-\alpha\tan\varphi}{2\beta}\left[\left(1 - 2\frac{\beta^2}{\alpha^2}\sin^2\theta + 2\frac{\beta}{\alpha}\cos\theta\cos\varphi\right)\right]$$

$$B_s = \frac{\alpha\tan\varphi}{2\beta}\left(4\frac{\beta^2}{\alpha^2}\sin^2\theta - 4\frac{\beta}{\alpha}\cos\theta\cos\varphi\right)$$

These equations can be put in the form:

$$AX = B \qquad (2.36)$$

where, X is a column vector of size 3x1, its elements being the three unknowns, $\Delta\rho/\rho, \Delta\alpha/\alpha$ and $\Delta\beta/\beta$;B is a column vector of size nx1, which are the n values of R_{pp} corresponding to n offsets, and A is a matrix of size nx3, its elements being the coefficients of $\Delta\rho/\rho, \Delta\alpha/\alpha$ and $\Delta\beta/\beta$ in (2.27)

Since, the above system is over determined; it is solved by using the least squares solution to the problem, thus giving the solution

$$X = \left(A^T A\right)^{-1} A^T B \qquad (2.37)$$

Traditionally, AVO methods rely on using only the PP wave reflectivity in order to obtain the properties $\Delta\rho/\rho, \Delta\alpha/\alpha$ and $\Delta\beta/\beta$. However, in recent times, the acquisition of PS data sets has found to be useful in providing additional information to represent the subsurface. In order to evaluate the usefulness of the PS data set for AVO, inversion of the PS synthetic gather was also carried out in the same way, as explained for the PP synthetic gather.

Similar procedure can be followed to obtain values of $\Delta\rho/\rho$ and $\Delta\beta/\beta$ (equation 2.28) by obtaining the values of R_{ps} from the PS synthetic seismogram for different offsets. In this case, the vector X is of size 2x1 and A is of size nx2. From these ratios, the velocities of P and S waves and densities above and below the interface can be determined.

2.7 Joint PP and PS Inversion Proposed by Stewart (1990)

In addition to performing the inversion for PS synthetic gather separately, a method for jointly inverting the PP and PS synthetic gather proposed by Stewart (1990) was also tested. The joint inversion scheme proposed by Stewart (1990) is as follows:

Equations (2.27) and (2.28) proposed by Aki and Richards can be simplified by using the Gardner's relationship (Gardner et al., 1974)

$$\rho = k\alpha^{1/4} \qquad (2.38)$$

which, when written in differential form becomes

$$\frac{\Delta\rho}{\rho} = \frac{1}{4}\frac{\Delta\alpha}{\alpha} \qquad (2.39)$$

Substituting equation (2.38) in the Aki and Richards approximations (2.27) and (2.28) leads to,

$$R^{pp}(\theta) \sim a\frac{\Delta\alpha}{\alpha} + b\frac{\Delta\beta}{\beta} \qquad (2.40)$$

$$R^{ps}(\theta) \sim c\frac{\Delta\alpha}{\alpha} + d\frac{\Delta\beta}{\beta} \qquad (2.41)$$

where,

$$a = \frac{1}{8}\left(1 - 4\frac{\beta^2}{\alpha^2}\sin^2\theta + \frac{4}{\cos^2\theta}\right)$$

$$b = -4\frac{\beta^2}{\alpha^2}\sin^2\theta$$

and

$$c = \frac{-\alpha\tan\varphi}{8\beta}\left(1 - 2\frac{\beta^2}{\alpha^2}\sin^2\theta + 2\frac{\beta}{\alpha}\cos\theta\cos\varphi\right)$$

$$d = \frac{\alpha\tan\varphi}{2\beta}\left(4\frac{\beta^2}{\alpha^2}\sin^2\theta - 4\frac{\beta}{\alpha}\cos\theta\cos\varphi\right)$$

The values of parameters $\Delta\alpha/\alpha$ and $\Delta\beta/\beta$ can be found by minimizing the objective function ε by least squares method (Stewart, 1990)

$$\varepsilon = \sum_{i=1}^{\#offsets}\left(R^{pp}(\theta) - a\frac{\Delta\alpha}{\alpha} - b\frac{\Delta\beta}{\beta}\right)^2 + \left(R^{ps}(\theta) - c\frac{\Delta\alpha}{\alpha} - d\frac{\Delta\beta}{\beta}\right)^2 \qquad (2.42)$$

17

The above method was a joint inversion method involving two parameters, $\Delta\alpha/\alpha$ and $\Delta\beta/\beta$. Based on this, a slight modification was done of the above method in order to yield a three term joint inversion involving three parameters $\Delta\rho/\rho$, $\Delta\alpha/\alpha$ and $\Delta\beta/\beta$ in the inversion. This is represented in the next section. For the purpose of this thesis, this method has been referred to as the two term joint inversion method

2.8 Modified Joint Inversion method.

The Gardener et al. (1974) relation, which was used to simplify the Aki Richards approximation in the previous section may not hold true in all cases and based on this thought, a slight modification was performed of the joint inversion method proposed by Stewart (1990)

Based on the Aki Richards approximations (2.27) and (2.28), the objective function for jointly inverting the PP and the PS synthetic gather can be represented as follows:

$$\varepsilon = \sum_{i=1}^{\#offsets} \left(R^{pp}(\theta) - A_p \frac{\Delta\alpha}{\alpha} - B_p \frac{\Delta\beta}{\beta} - C_p \frac{\Delta\rho}{\rho} \right)^2 + \left(R^{ps}(\theta) - A_s \frac{\Delta\rho}{\rho} - B_s \frac{\Delta\beta}{\beta} \right)^2 \qquad (2.43)$$

Minimizing (2.43) leads to a three term joint inversion method, yielding values of $\Delta\rho/\rho$, $\Delta\alpha/\alpha$ and $\Delta\beta/\beta$. For the purpose of this thesis, this method has been referred to as the Modified Joint Inversion Method.

CHAPTER 3

COMPUTATIONAL ASPECTS

3.1 Introduction

In this dissertation, synthetic seismograms have been generated for a number of three layered models. Both PP and PS synthetic seismograms have been generated. A plane P – wave is emitted from a source lying on the free surface and reflected P and S wave amplitudes have been computed at a number of geophone locations at the free surface. Reflection coefficients at non normal incidence, at the interfaces have been computed using the formulation based on Zoeppritz equations.

The amplitudes of P and S waves on synthetic seismograms have been treated as field data in a CMP gather and inverted to obtain the layer parameters using approximations to Zoeppritz equations proposed by Aki and Richards (2002). Joint inversion schemes have also been used for the same purpose and the results of different inversion schemes have been compared.

3.2 Sequential Execution of Work.

A) Forward Modelling (Generation of Synthetic Seismograms)

1) A three layered earth model has been chosen in the manner as described below. Several lithological models have been obtained from the literature, containing different fluid contents. Each model consists of three layers and each layer has been assumed to be homogeneous and isotropic. In each model, the thickness of the first layer is assumed to be an elastic shale layer with thickness of 1800 metres. The second layer is assumed to be a reservoir rock with a thickness of 100 metres and can be saturated with brine, oil or gas. The third layer is assumed to be an elastic infinite half space. Each layer is defined by prescribing a P wave velocity, an S wave velocity and a density. For the purpose of this study, the values of these parameters have been obtained from the field models described in Engelmark (2001). The details of different models are given in table 4.1
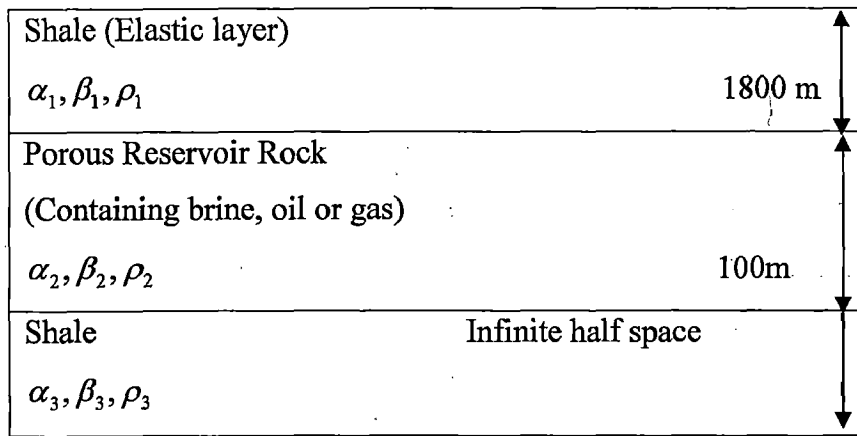
Shale (Elastic layer) $\alpha_1, \beta_1, \rho_1$	1800 m
Porous Reservoir Rock (Containing brine, oil or gas) $\alpha_2, \beta_2, \rho_2$	100m
Shale Infinite half space $\alpha_3, \beta_3, \rho_3$	

Figure 3.1: A typical model used for the study.

2) Once the model is chosen, the aim is to construct a synthetic seismogram. Source - receiver distances are so chosen to cover a range of incidence angles from $0°$ to $30°$. This is because, as reported by Castagna (1993), the approximations to the Zoeppritz equations cannot be extended beyond $30°$ of angle of incidence. The Aki – Richards' approximation to the Zoeppritz equation has been used for the purpose of inverting the synthetic data set. Hence the study considers incidence angles only upto a range of $0°$ to $30°$. The corresponding maximum offset is about 1000 metres.

3) The next step is to compute the angle i, at which the ray is incident at the interface so as to return, after reflection at the geophone location at the given distance. The source is placed at the surface z = 0, is assumed to emit plane waves of unit amplitude. This problem is solved separately for reflected P wave and reflected S wave, as seen in Figure 3.2.

4) For the above model setting, ray tracing is performed for each particular model. Ray tracing is used in calculating the required ray path for a particular source and geophone setting and using the concept of Snell's Law. The final output after ray tracing is to obtain the angle of incidence and the travel time of the ray from the source to all the receivers. The ray tracing for a particular model for PP and PS waves are shown in Figure 3.3.
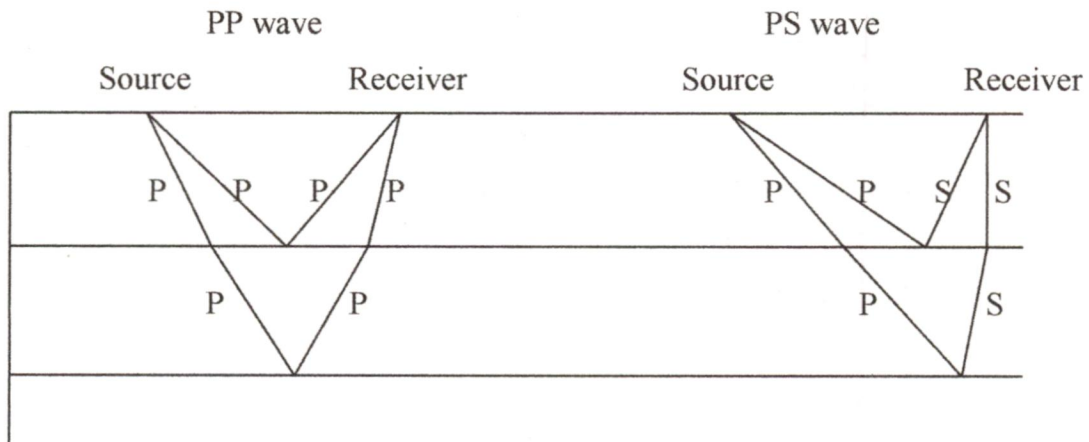
PP wave

PS wave

Source   Receiver   Source   Receiver

P   P   P   P   P   P   S   S

P   P   P   S

Figure 3.2: Synthetic PP and PS seismogram ray paths for a single source – receiver pair.
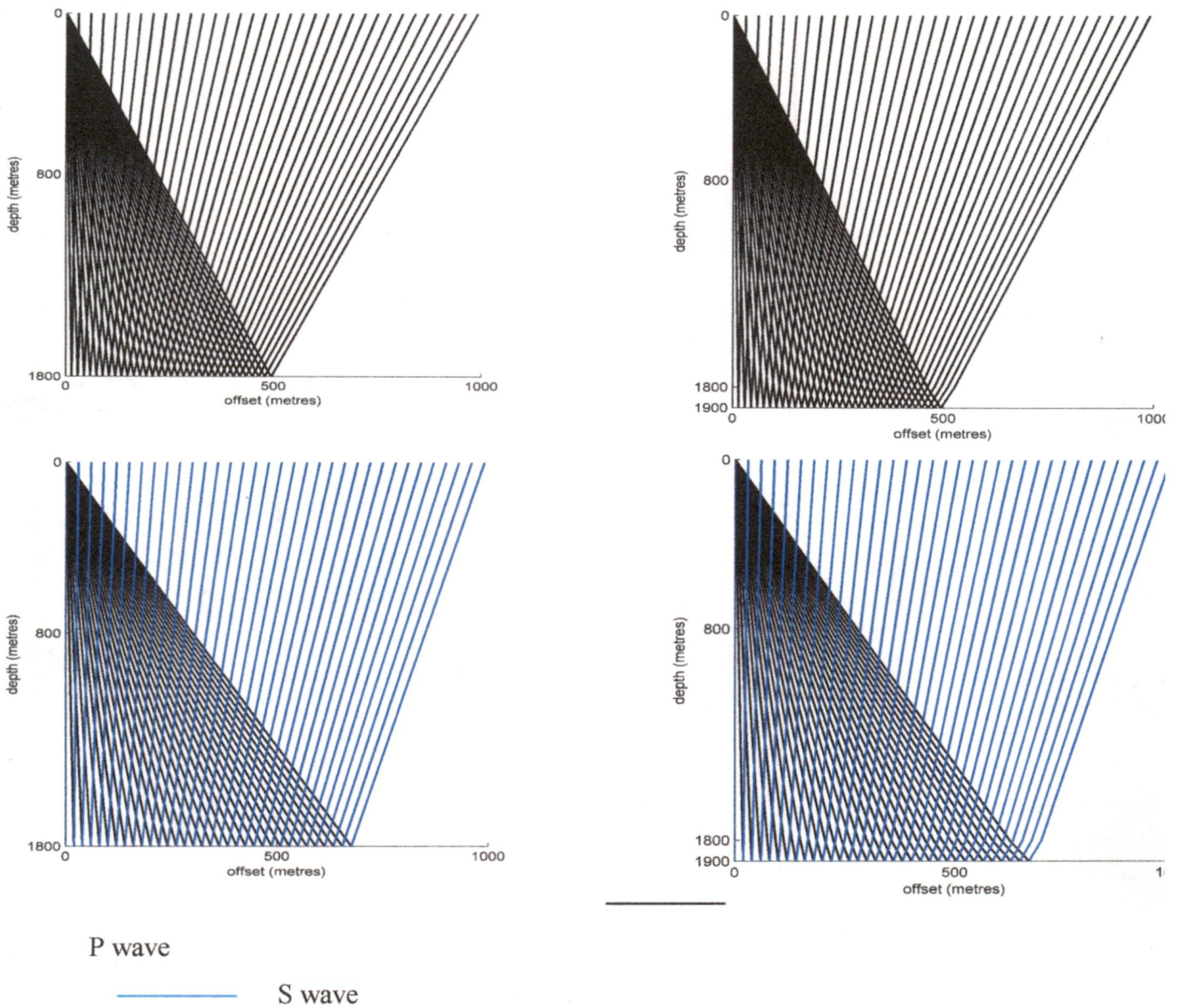
P wave

———————   S wave

Figure 3.3: Ray tracing for the PP and PS ray paths for a particular model in Figure 3.1

21

5) The P wave incident at an interface is reflected and transmitted to give four new waves. It is required to compute amplitudes of reflected P and reflected S waves at each interface. This requires computation of reflection coefficients, which is the next step performed.

6) Synthetic seismograms have been computed using relations (2.33) and (2.34). These are reproduced below:

For reflected P waves

$$U_z(0,t) = \left\{ \frac{-2\dfrac{\alpha}{\beta^2}\dfrac{\cos i}{\alpha}\left(\dfrac{1}{\beta^2}-2p^2\right)}{\left[\left(\dfrac{1}{\beta^2}-2p^2\right)^2 + 4p^2 \dfrac{\cos i}{\alpha}\dfrac{\cos j}{\beta}\right]} \right\} \text{x Product x } R_{pp} \text{ x exp (t - Sum)}$$

For reflected S waves

$$U_r(0,t) = \left\{ \frac{4\dfrac{p}{\beta}\dfrac{\cos i}{\alpha}\dfrac{\cos j}{\beta}}{\left[\left(\dfrac{1}{\beta^2}-2p^2\right)^2 + 4p^2 \dfrac{\cos i}{\alpha}\dfrac{\cos j}{\beta}\right]} \right\} \text{x Product x } R_{ps} \text{ x exp (t - Sum)}$$

7) The reflection and the transmission coefficients $R_{pp}, R_{ps}, T_{pp}, T_{ps}$ have been computed for different angles of incidence by solving the set of simultaneous equations (2.17) and (2.18) and reproduced below

MX = N

where, M is given by equation (2.17) and N is a column vector given in equation (2.18). X is a column of unknown coefficients $R_{pp}, R_{ps}, T_{pp}, T_{ps}$.

8) Once the reflected P and reflected S waves emerge from the interfaces, these reach the surface to be recorded at the appropriate geophone location. Before these amplitudes are picked up by the geophone at the free surface, the effect of free needs to be computed. The reflection coefficients $R_{pp}, R_{ps}, T_{pp}, T_{ps}$ obtained, are multiplied by a factor to account for the free surface effect, as given in equations

(2.33) and (2.34) and the reflectivity series is formed. The reflectivity series is then convolved with a Ricker wavelet of 50 Hz to obtain the synthetic seismogram (Sheriff, 2002).

9) The above exercise is repeated at all the geophone locations giving the synthetic seismogram to yield the PP and PS synthetic seismograms at all the receiver locations.

B) Inversion of the obtained reflection coefficients for the first reflector in the synthetic seismogram using the Aki Richards approximation.

1) The amplitudes of reflected waves on synthetic seismograms are considered as raw data for the purpose of inversion, using various approximations to Zoeppritz equations. The maximum amplitudes of the reflected pulses are equal to amplitudes of reflected P and S waves modified by the free surface effect. This effect is removed before inversion. The inversion is applied to seismograms generated corresponding to the first interface only. The angle of incidence is obtained from knowledge of offset (X) and depth to the interface, by using ray tracing. On removing the free surface effect, the corrected amplitudes are reflection coefficients at different angles of incidence. These reflection coefficients are then inverted to get layer parameters (P and S wave velocity and density).

2) The inversion is performed for the first interface of the PP synthetic gather as outlined in the Chapter 2 by using the equation (2.36), reproduced below:

$$X = \left(A^T A\right)^{-1} A^T B$$

X is a column vector of size 3x1, its elements being the three unknowns, $\Delta\rho/\rho$, $\Delta\alpha/\alpha$ and $\Delta\beta/\beta$; B is a column vector of size nx1, which are the n values of R_{pp} corresponding to n offsets, and A is a matrix of size nx3, its elements being the coefficients of $\Delta\rho/\rho$, $\Delta\alpha/\alpha$ and $\Delta\beta/\beta$ in (2.25).

3) The above inversion requires some background value of the ratio α/β. Different values of α/β are input into the inversion, such that the errors are less than 10%. Once an appropriate value of α/β is input into the inversion, the values of $\Delta\rho/\rho, \Delta\alpha/\alpha$ and $\Delta\beta/\beta$ are obtained.

4) An estimate of α is obtained by fitting a straight line to the square of the two-way travel times versus square of offsets ($t^2 - x^2$ method of velocity determination). Estimate of β is obtained by dividing α by an appropriate value of α/β. The mean density ρ is given an appropriate value.

5) From the values of $\Delta\rho/\rho$, $\Delta\alpha/\alpha$ and $\Delta\beta/\beta$, and ρ, β and α so obtained, the estimates of the P and the S wave velocities and densities are obtained for the first two layers in the model.

6) The inverted values are compared with the actual model values and the relative percent errors determined.

7) The same procedure is repeated for the PS synthetic gather.

C) Inversion of the obtained reflection coefficients for the first reflector in the synthetic seismogram using the joint inversion method proposed by Stewart (1990):

1) The inversion is performed by minimizing the objective function by the method of least squares (equation 2.42).

$$\varepsilon = \sum_{i=1}^{\#offsets}\left(R^{PP}(\theta) - a\frac{\Delta\alpha}{\alpha} - b\frac{\Delta\beta}{\beta}\right)^2 + \left(R^{Ps}(\theta) - c\frac{\Delta\alpha}{\alpha} - d\frac{\Delta\beta}{\beta}\right)^2$$

2) The input values of α/β and the estimates of ρ, β and α are obtained in the same manner as in the previous inversion method

3) From the values of $\Delta\rho/\rho, \Delta\alpha/\alpha$ and $\Delta\beta/\beta$, and ρ, β and α so obtained, the estimates of the P and the S wave velocities and densities are obtained for the first two layers in the model and the relative % errors are calculated.

D) Inversion of the obtained reflection coefficients for the first reflector in the synthetic seismogram using the modified joint inversion method explained in Chapter 2.

1) The inversion is performed by minimizing the objective function by the method of least squares (equation 2.43).

$$\varepsilon = \sum_{i=1}^{\#offsets} \left(R^{pp}(\theta) - A_p \frac{\Delta\alpha}{\alpha} - B_p \frac{\Delta\beta}{\beta} - C_p \frac{\Delta\rho}{\rho} \right)^2 + \left(R^{ps}(\theta) - A_s \frac{\Delta\rho}{\rho} - B_s \frac{\Delta\beta}{\beta} \right)^2$$

2) The input values of α/β and the estimates of ρ, β and α are obtained in the same manner as in the previous inversion method.

3) From the values of $\Delta\rho/\rho$, $\Delta\alpha/\alpha$ and $\Delta\beta/\beta$, and ρ, β and α so obtained, the estimates of the P and the S wave velocities and densities are obtained for the first two layers in the model and the relative % errors are calculated.

3.3 Computer Programs

The following computer programs have been written for this thesis.

1) Ray tracing code for PP and PS ray paths and travel times.

2) Computation of reflection and transmission coefficients and the free surface effect for various angles of incidence for PP and PS.

3) Generation of synthetic seismograms for PP and PS.

4) Estimate of P wave velocity in first layer by $t^2 - x^2$ method.

5) Correcting the amplitudes for free surface effect.

6) Inversion code using Aki Richards approximations for PP and PS.

7) Inversion code using joint inversion method by Stewart (1990).

8) Inversion code for modified joint inversion method.

All the above programs have been written in MATLAB.
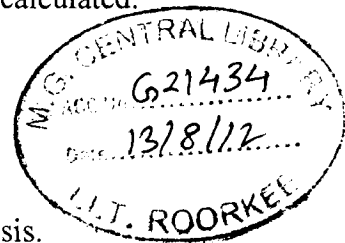
CHAPTER 4

RESULTS AND DISCUSSIONS

4.1 Generation of Synthetic Seismograms

Synthetic seismograms have been generated on the surface three layered Earth models. The model consists of a reservoir rock sandwiched between two shale layers. The model shown in Figure 4.1 is reproduced here.

Shale (Elastic layer) $\alpha_1, \beta_1, \rho_1$		1800 m
Reservoir Rock	$\alpha_2, \beta_2, \rho_2$	100m
Shale $\alpha_3, \beta_3, \rho_3$	Infinite half space	

Figure 4.1: A typical model used for the study.

For the purpose of this study, several models have been adopted from Engelmark (2001). Table 4.1 shows the parameters for the various lithological models that have been used in the study.

The values of the ratios $\Delta\rho/\rho, \Delta\alpha/\alpha$ and $\Delta\beta/\beta$ for the first two layers have been calculated before hand for each model to gain an idea of the original contrasts present in ρ, β and α. These have been tabulated in Table 4.2. The absolute values of these contrasts are presented in Figure 4.3.

As can be seen in Figure 4.3, the contrasts in beta (absolute values of $\Delta\beta/\beta$) are the highest for all the models. Also, for the models to the right of model 3C, the contrasts (absolute values of $\Delta\rho/\rho, \Delta\alpha/\alpha$ and $\Delta\beta/\beta$) are comparatively higher than the models to the left of model 3C. The values of $\Delta\rho/\rho, \Delta\alpha/\alpha$ and $\Delta\beta/\beta$ in the original models are important to evaluate and explain the inversion results, as discussed later.

Synthetic Seismograms have been generated at 34 receiver locations with receiver interval equal to 30 m. A plane wave of unit amplitude starts from the source S at the free surface and travels downward into the earth model. Reflections take place at the upper and lower

boundary of the reservoir layer and the vertical (PP) and horizontal (PS) components of each reflection are evaluated at the 34 receiver locations from each interface. The method of computing the synthetic seismograms has been presented in Chapter 3.

Model 1 comprises of a shale layer overlying a gas sand layer. Figure 4.4 shows the PP and the PS synthetic seismograms generated for this model. For the first interface, the PP seismograms first show a decrease followed by an increase in the amplitude with offset. There is also a change in the polarity. The PS seismograms show an increase in the amplitude with offset for the first interface.

Models 2A, 2B and 2C consist of a shale layer overlying a sandstone layer with 30% porosity, saturated with 100% brine, 90% oil and 90% gas respectively. Figure 4.5, 4.6, 4.7 show the PP and the PS synthetic seismograms generated for this group of models. For the first interface, the PS seismograms for the above group of models show an increase in amplitude with offset. The PP seismograms for model 2A show a decrease in amplitude with offset whereas for models 2B and 2C, there is an increase accompanied with a change of polarity.

Models 3A, 3B, 3C consist of a group of models wherein, shale overlies brine saturated sandstone with 30 %, 33.6% and 35.6% porosities respectively. Figures 4.8, 4.9, 4.10 show the PP and the PS synthetic seismograms generated for this group of models For the first interface, the PS seismograms for the above group of models show amplitude increase with offset. The polarity is reverse for model 3B. The PP seismograms for model 3A show a decreasing trend, whereas for models 3B and 3C, amplitude increases with offset with reverse polarity for model 3C.

Models 4A, 4B, 4C have different kinds of shales overlying 90% oil saturated sand. Figures 4.11, 4.12, 4.13 show the PP and the PS synthetic seismograms generated for this group of models The overlying shales are specified as soft, medium and hard characterized by increasing seismic velocities. For the first interface, the PS seismograms for the above group of models show an amplitude increase with offset. The PP seismograms for model 4A show a decreasing trend, whereas for models 4B and 4C, an amplitude increase with offset is observed. There is a reverse polarity for models 4B and 4C.

Model 5 consists of gas saturated sand overlying shale. Figure 4.14 shows the PP and the PS synthetic seismograms generated for this model. For the first interface, both the PP and the PS seismograms show increasing amplitude with offset. The polarity for PP seismograms is reverse.

4.2 Inversion of Synthetic Seismograms for the first interface.

Synthetic Seismograms for a number of earth models have been generated and inverted following the procedures outlined in Chapter 3. This has yielded P and S wave velocities and densities above and below the first reflector. Relative percentages errors have been computed between the actual and inverted values and tabulated for different models. The relative errors for the properties of the first two layers using the various methodologies have been presented in Figures 4.15, 4.16 and 4.17 and been placed in the Appendix.

One significant result observed by comparing Figure 4.2 with Figures 4.15, 4.16, 4.17, is that the errors are lower in those portions of the Figures 4.15, 4.16, 4.17 which correspond to lower contrasts in the properties (lower absolute values of $\Delta\rho/\rho, \Delta\alpha/\alpha$ and $\Delta\beta/\beta$) in Figure 4.3.

4.3 Discussion

The inversion is carried out on PP and PS reflection coefficients which have been extracted from the seismograms.

The inversion for P-wave velocities as been carried out using PP-inversion, Stewart method and modified Stewart's method. The latter two methods are joint inversion methods that make use of both PP and PS coefficients. The results have been shown in Figure 4.15. In the Stewart's method expressions for PP and PS coefficients have been simplified using Gardner's relation. This reduces the number of model parameters to be determined from three to two. It is expected that this will lead to greater accuracy in the values of the inverted parameters. In the modified Stewart's method, no simplification of expressions for PP and PS coefficients has been made.

The inversion for densities has been carried out using PP and PS inversion, Stewart's method and modified Stewart's method of joint inversion. The results are shown in Figure 4.16.

28

The inversion for S wave velocities has been carried out using PP and PS inversion along with the two joint inversion methods. The results are shown in Figure 4.17.

The Stewart's method (two term joint inversion) gives smaller errors when contrasts in ρ, β and α are low. When these become large, the modified Stewart's method (three term joint inversion) seems to be better.

A) PP vs. PS inversion using Aki Richards approximations

From the Figures 4.16 and 4.17, it is clearly seen that for all the inversion results, PS inversion for density and S wave velocity gives a higher error than PP. This is basically because of the fact that the Aki Richards approximation for PS coefficient shows a larger deviation from the exact results (Zoeppritz equations) than the approximation for PP coefficients. This leads to higher errors in the PS inversion. (Aki and Richards, 2002). This can be seen in Figure 4.2 for model 2C.
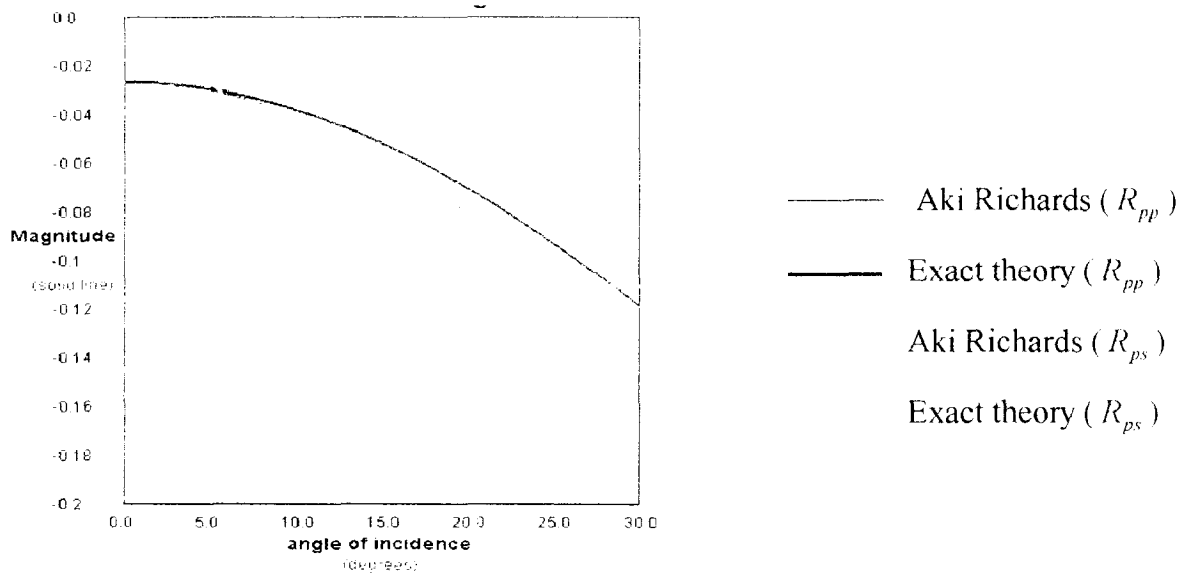
Figure 4.2: R_{pp} and R_{ps} for model 2C, using exact theory and Aki Richards approximations.

B) Two Term joint inversion (Stewart, 1990) vs. Three Term joint inversion (Modified Joint Inversion)

From the Figures 4.15, 4.16 and 4.17, it is can be seen that the two term joint inversion (Stewart, 1990) gives better results than the modified three term joint

inversion method for P and S wave velocities and densities. The two term joint inversion method yields $\Delta\alpha/\alpha$ and $\Delta\beta/\beta$. Using Gardner's relation (equation 2.39) again, it is possible to get $\Delta\rho/\rho$ from $\Delta\alpha/\alpha$. Except in the case of inversion errors in β (Figure 4.17), the three term method gives better results than the two term inversion for models 4A onwards (those having a higher absolute value of the contrasts in Figure 4.3). This can be explained as follows: the two term method, involving one less parameter than the three term method should give better results. However, when the contrast between the adjacent layers becomes rather high, the two term approximation seems to be less accurate.

C) <u>Inversion errors in P wave velocity.</u>

From the Figure 4.15, it can be seen that the PP inversion gives the smallest errors in the P wave velocity in the inversion. However, as contrasts increase (towards the right of Figure 4.15, as seen from figure 4.3), either of the joint inversion methods gives a better result.

Thus for finding the P wave velocity, the PP data set is sufficient, however in cases of higher contrast, it may require additional information in the form of PS dataset.

D) <u>Inversion errors in the density</u>

From the figure 4.16, it can be seen that the PP inversion gives smallest the smallest errors in density inversion. However, when the contrast in the models increase towards the right hand side of the figure, the three term joint inversion is better. Thus for finding the density, the PP data set is sufficient, however in cases of higher contrast, it may require additional information from PS dataset.

E) <u>Inversion errors in the S wave velocity.</u>

The results for the S wave velocity inversion show different results from the other two. It can be seen from figure 4.17, that the errors in the S wave velocity are smallest for the two term joint inversion for lower contrasts (toward the left in the figure), and for the three term joint inversion for higher contrasts. The PS results are the least accurate for calculating the S wave velocity. Thus the joint use of a PP and a PS data set may help in providing a better estimate of the S wave velocity.

Model No.	Lithology	P-wave Velocity (m/sec)	S-wave Velocity (m/sec)	Density (g/cm^3)
1	Shale	2898	1290	2.42
	Gas Sand	2857	1666	2.27
	Shale	2898	1290	2.42
2A	Shale	2819	1441.70	2.35
	100% brine saturated sandstone	3400	2098.24	2.16
	Shale	2819	1441.70	2.35
2B	Shale	2819	1441.70	2.35
	90% oil saturated sandstone	3220	2147.30	2.06
	Shale	2819	1441.70	2.35
2C	Shale	2819	1441.70	2.35
	90% gas saturated sandstone	3234.8	2214	1.94
	Shale	2819	1441.70	2.35
3A	Shale	2819	1441.70	2.35
	30% porous sandstone	3400	2098.24	2.16
	Shale	2819	1441.70	2.35
3B	Shale	2819	1441.70	2.35
	33.6% porous sandstone	3160.4	1909.50	2.10
	Shale	2819	1441.70	2.35
3C	Shale	2819	1441.70	2.35
	35.6% porous sandstone	3033.9	1808	2.07
	Shale	2819	1441.70	2.35
4A	Soft Shale	2599	1269	2.31
	90% oil saturated sandstone	3220	2147	2.06
	Soft Shale	2599	1269	2.31
4B	Medium Shale	2819	1441	2.35
	90% oil saturated sandstone	3220	2147	2.06
	Medium Shale	2819	1441	2.35
4C	Hard Shale	2952	1546	2.38
	90% oil saturated sandstone	3220	2147	2.06
	Hard Shale	2952	1546	2.38
5	Shale	2590.8	1295.4	2.50
	Gas sand	1737.3	868.68	2.02
	Shale	2590.8	1295.4	2.50
6	Shale	2438.4	995.47	2.16
	Carbonate	3459.48	1849.16	2.20
	Shale	2438.4	995.47	2.16

Table 4.1 Parameters of different lithological models

model	$\Delta\alpha/\alpha$	$\Delta\beta/\beta$	$\Delta\rho/\rho$
1A	-0.014	0.254	-0.064
2A	0.187	0.371	-0.084
2B	0.133	0.393	-0.131
2C	0.137	0.422	-0.191
3A	0.186	0.371	-0.084
3B	0.114	0.279	-0.112
3C	0.073	0.225	-0.126
4A	0.213	0.514	-0.114
4B	0.133	0.393	-0.132
4C	0.087	0.326	-0.144
5	-0.394	-0.394	-0.212
6	0.346	0.600	0.018

Table 4.2: Values of $\Delta\rho/\rho$, $\Delta\alpha/\alpha$, $\Delta\beta/\beta$ in the original models for the first two layers
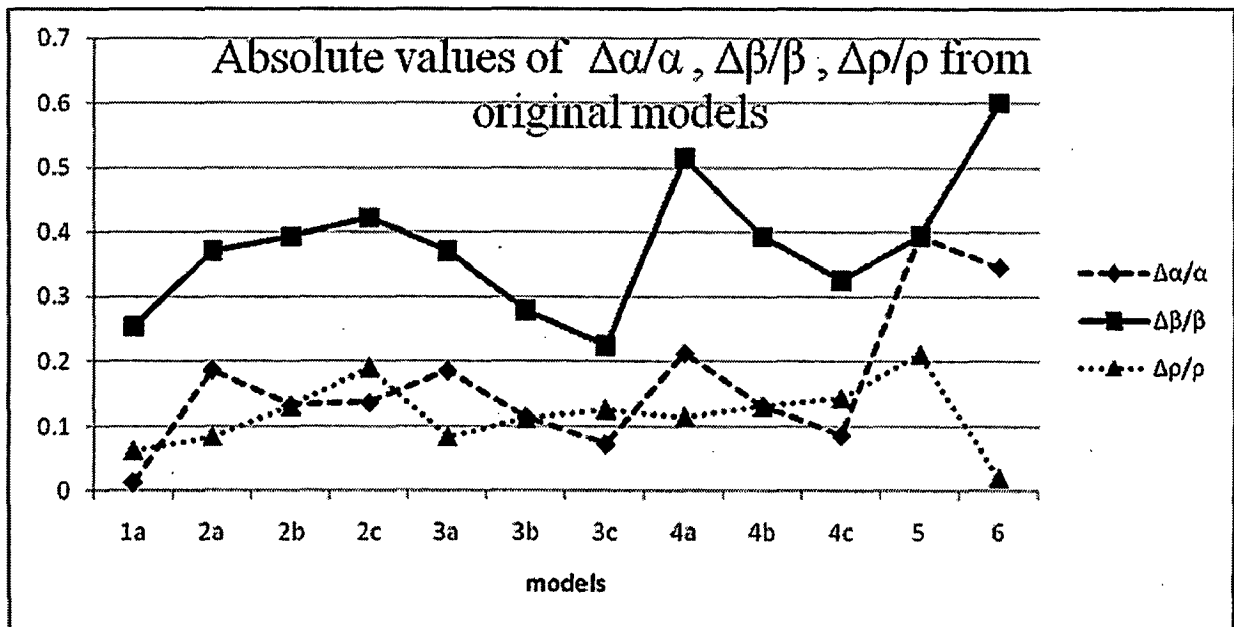
Figure 4.3: Absolute values of $\Delta\rho/\rho$, $\Delta\alpha/\alpha$, $\Delta\beta/\beta$ in the original models between the first two layers.
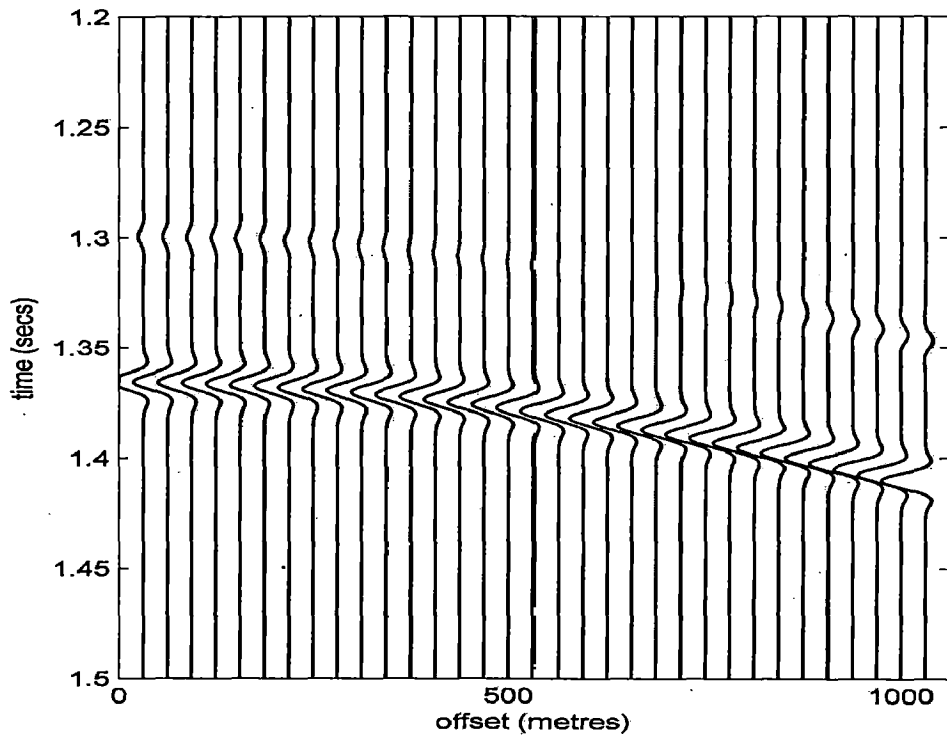
(A)
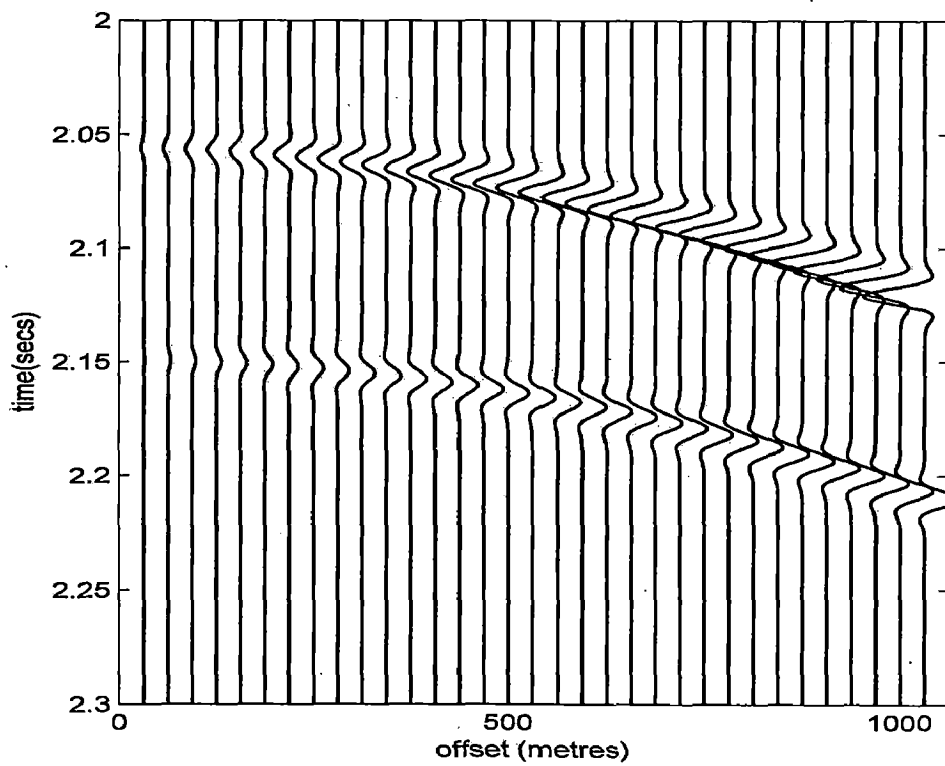
(B)

Figure 4.4 : Synthetic Seismogram for model 1   (A) – PP (B) - PS
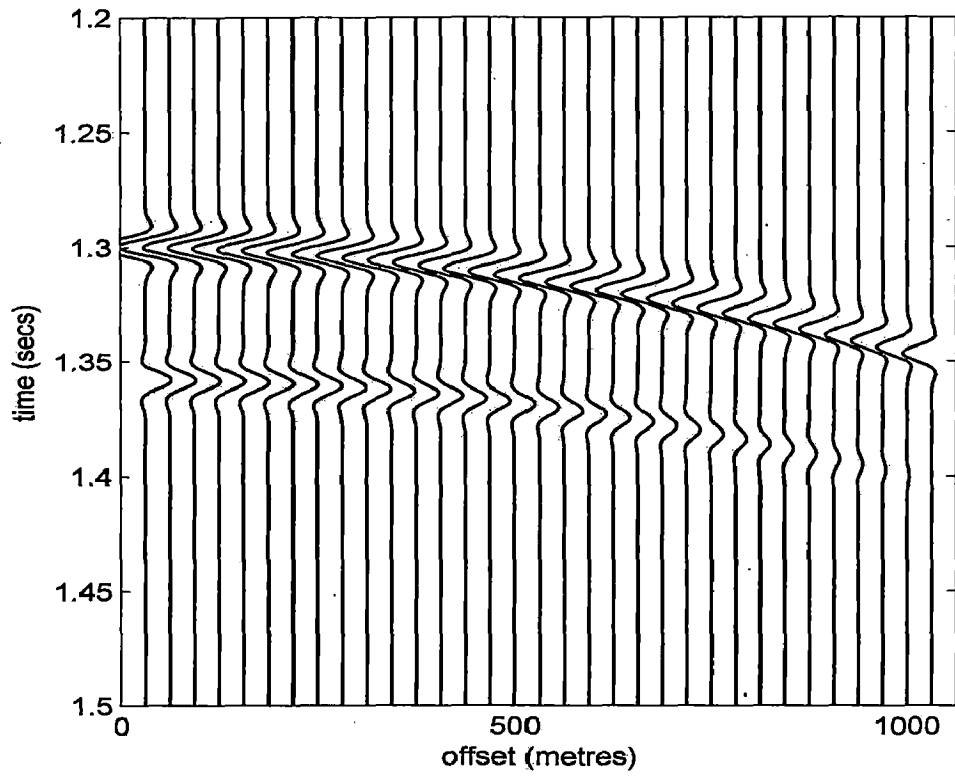
(A)
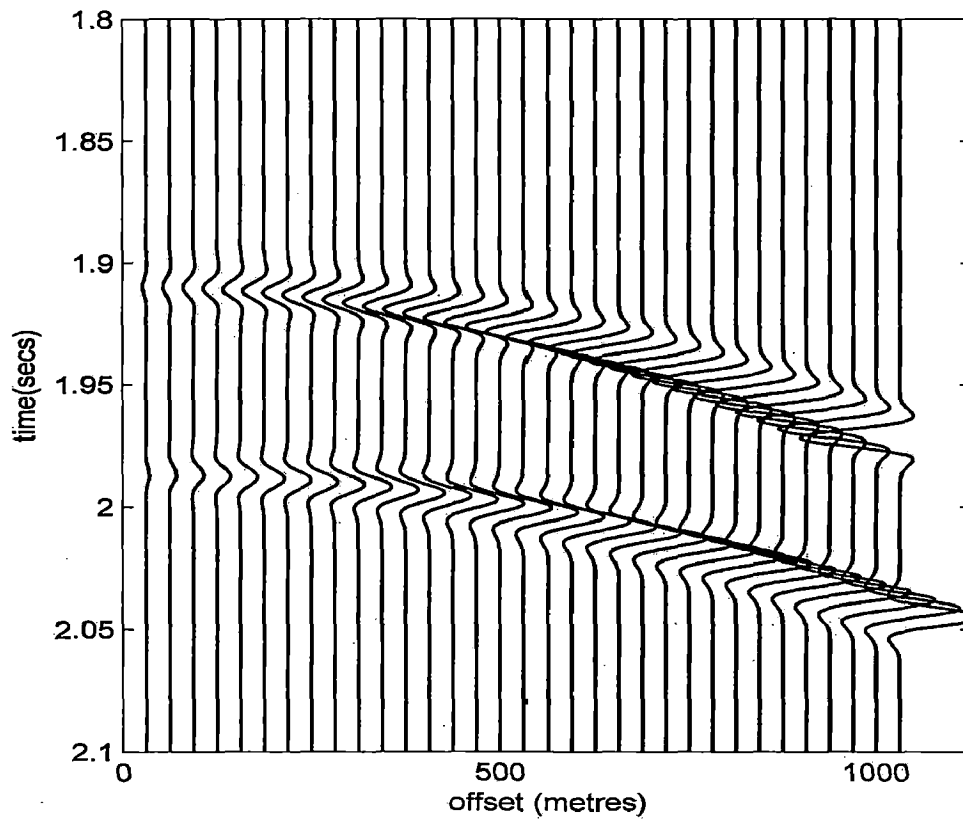
(B)

Figure 4.5 : Synthetic Seismogram for model 2A   (A) – PP (B) - PS
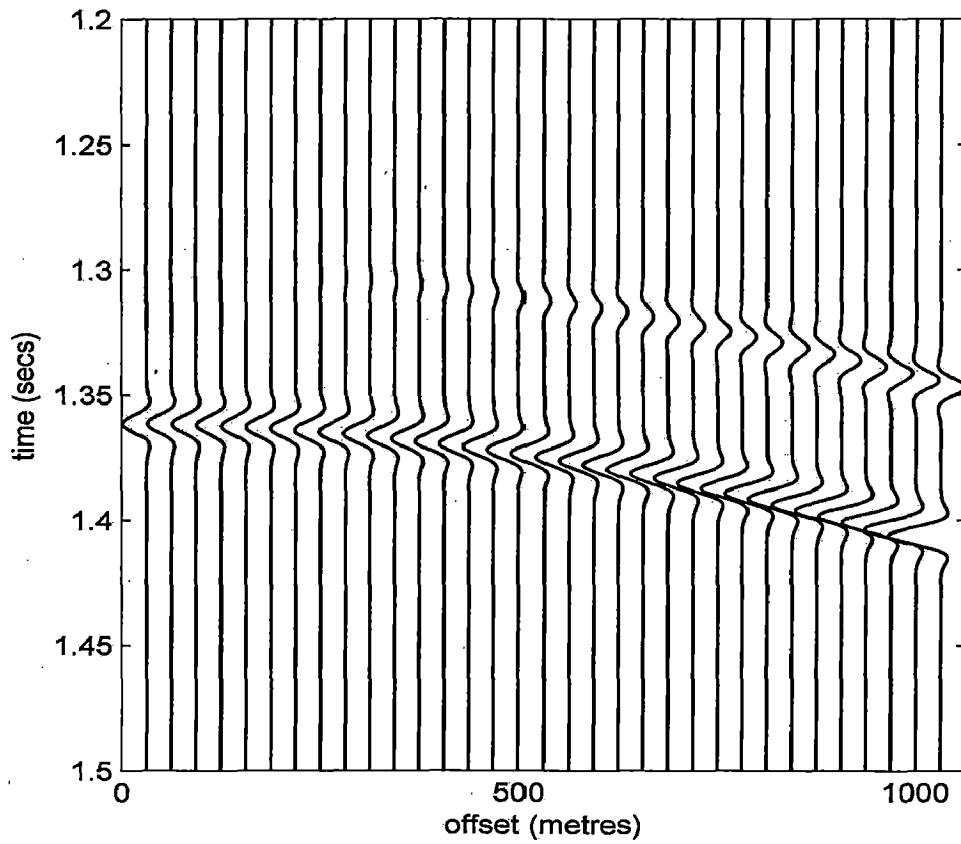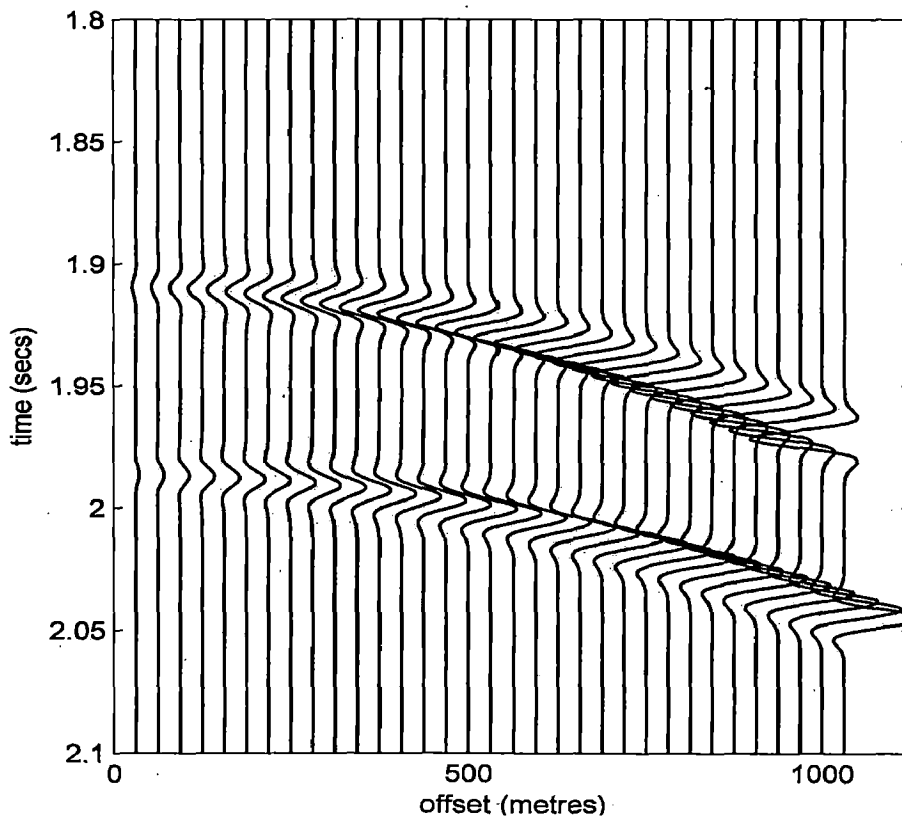
(A)
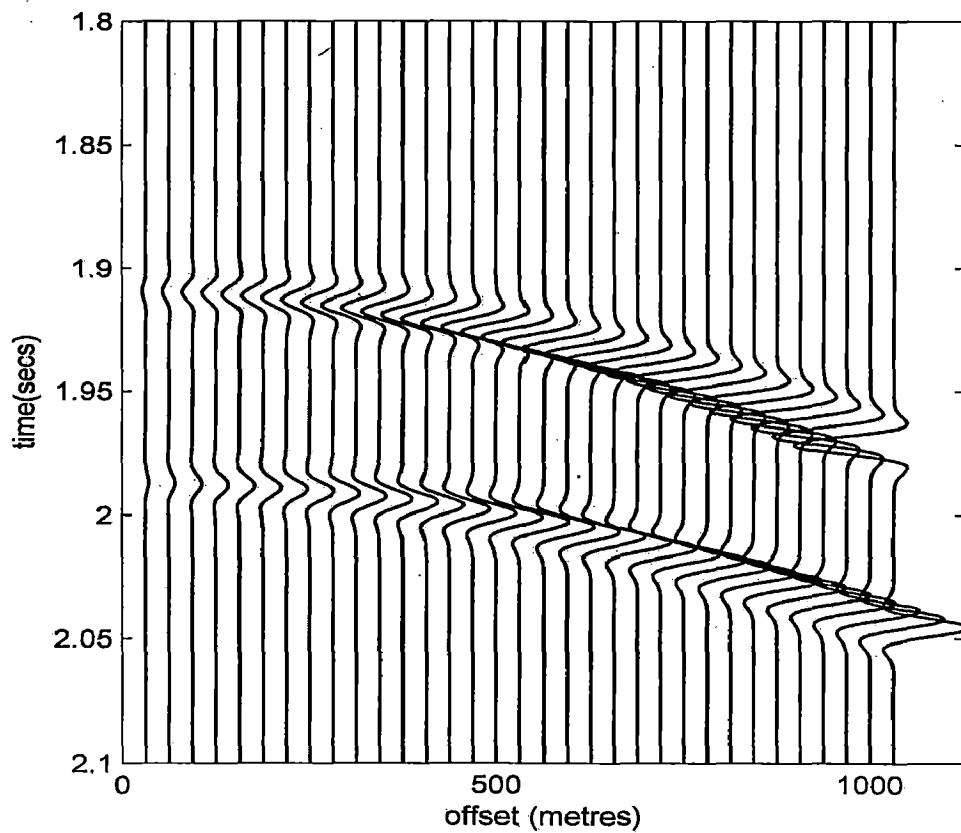
(B)

Figure 4.6 : Synthetic Seismogram for model 2B   (A) – PP (B) - PS

(A)
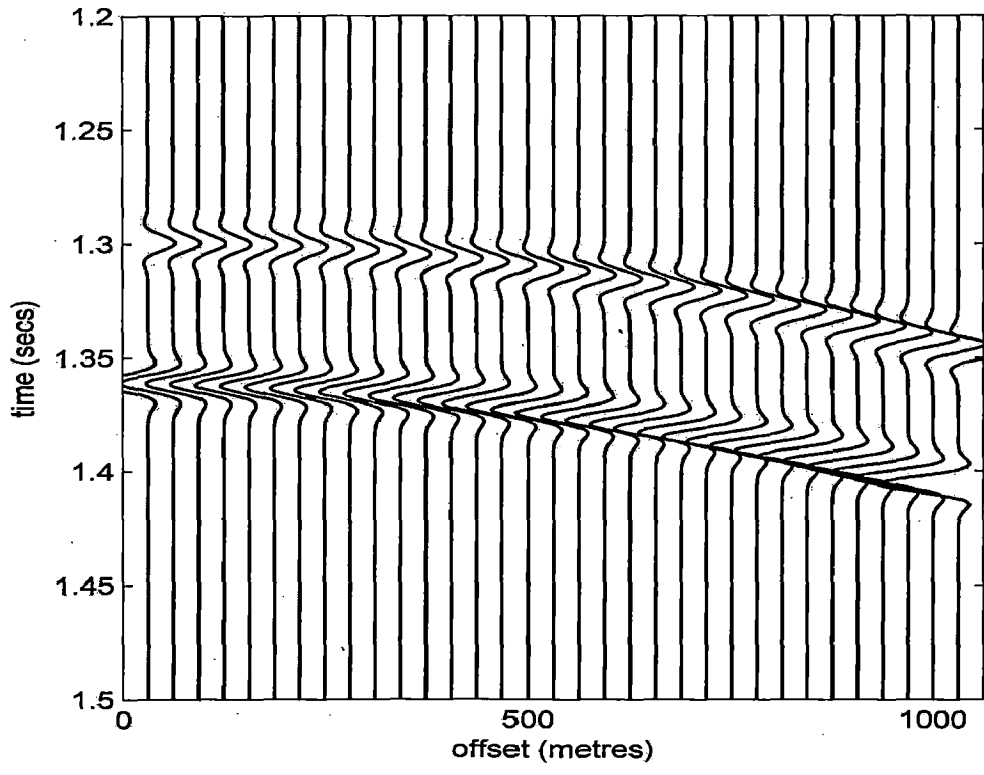
(A
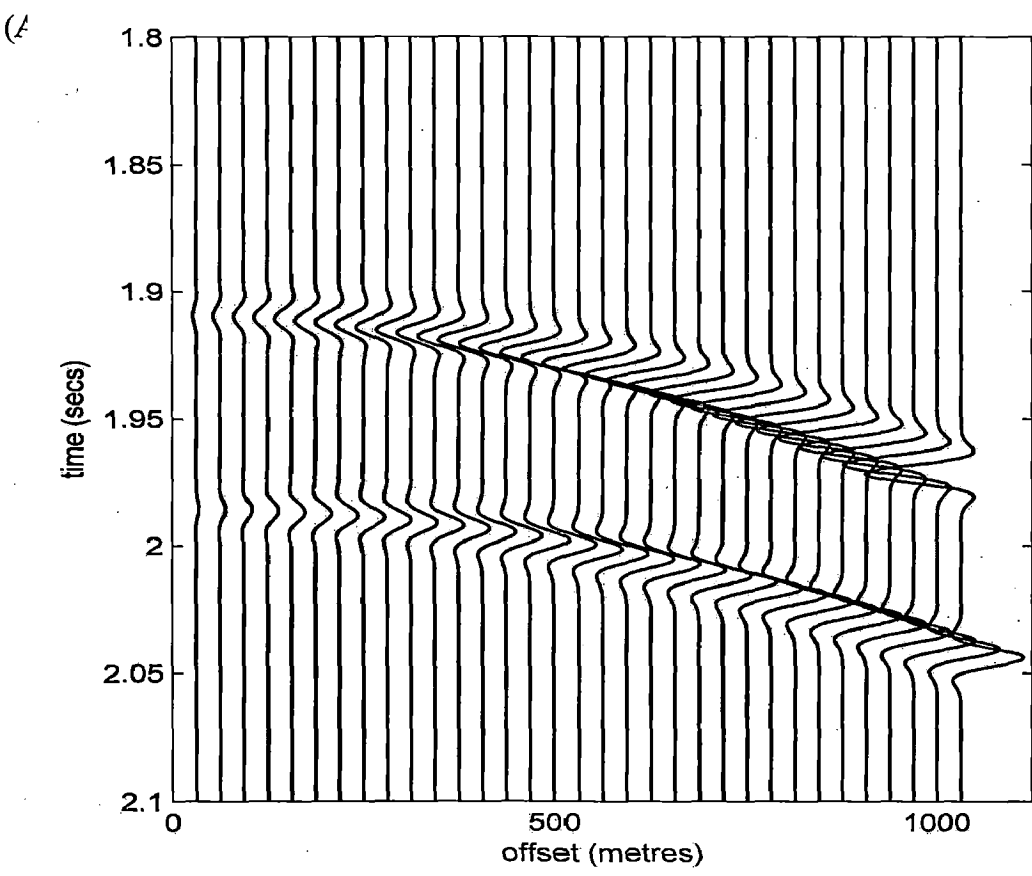
(B)

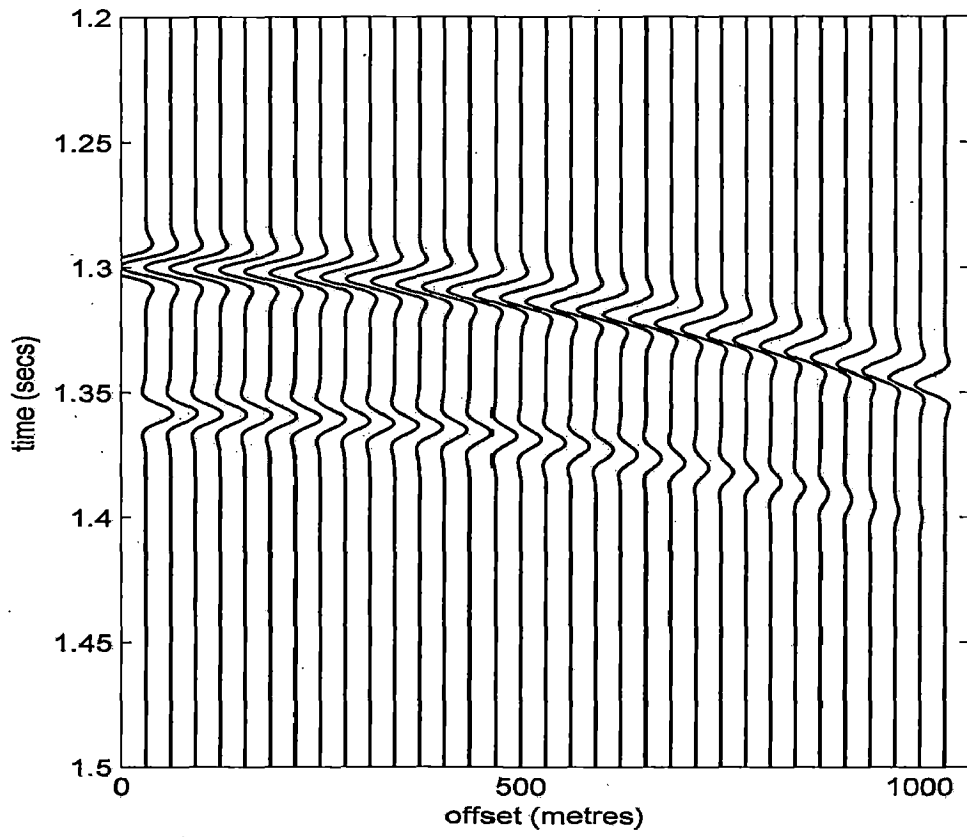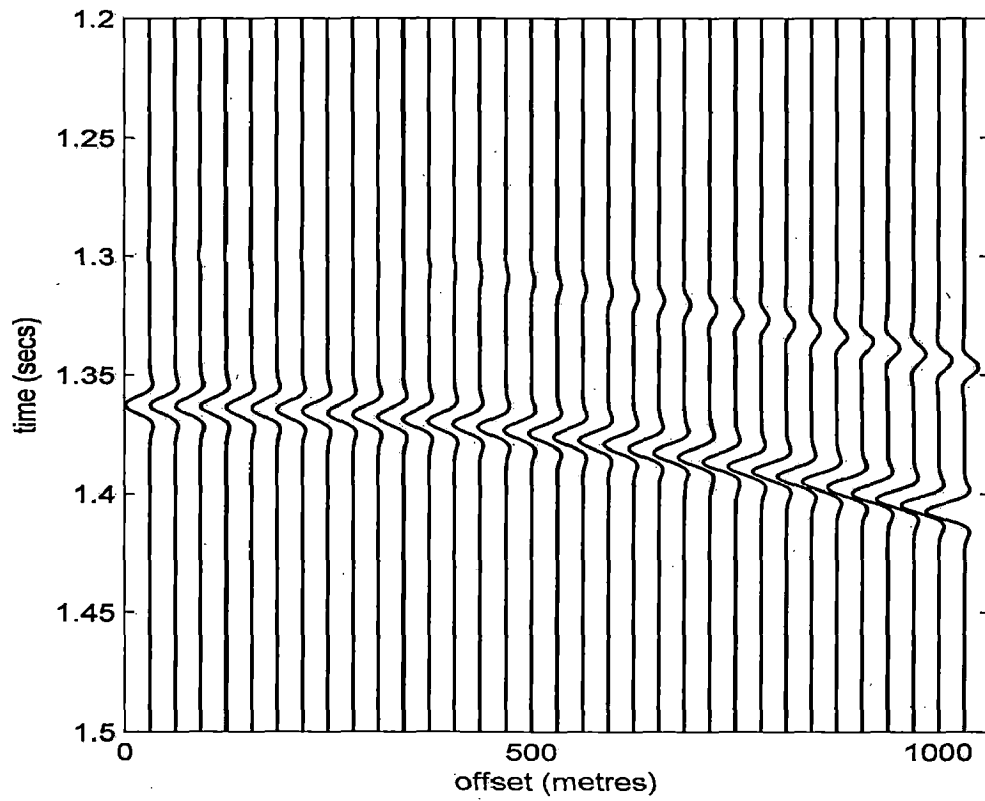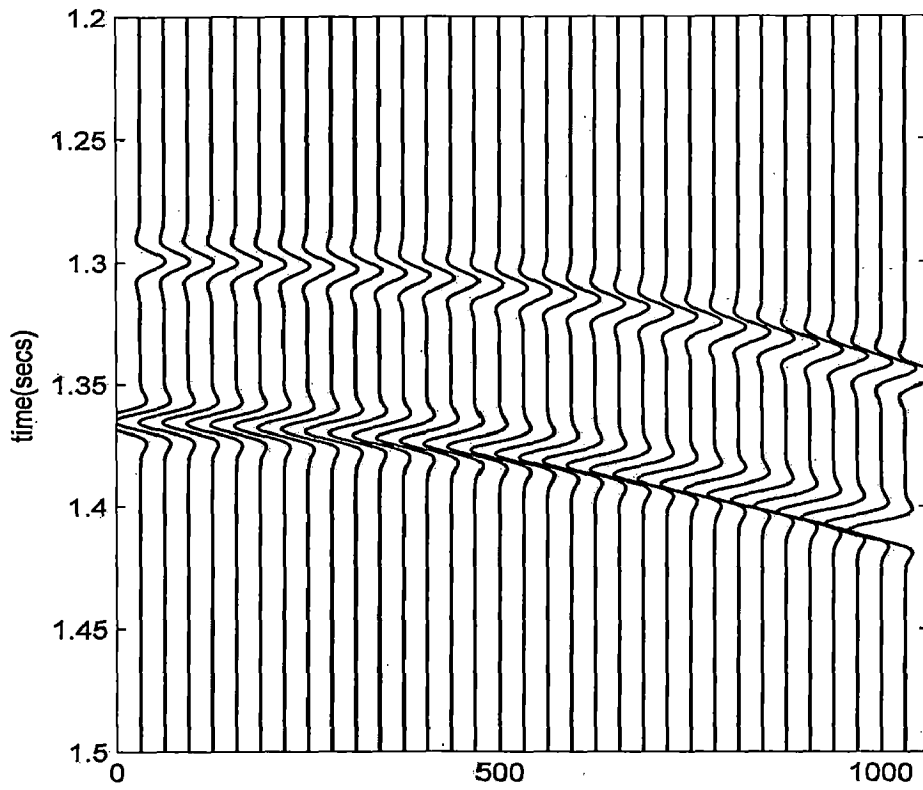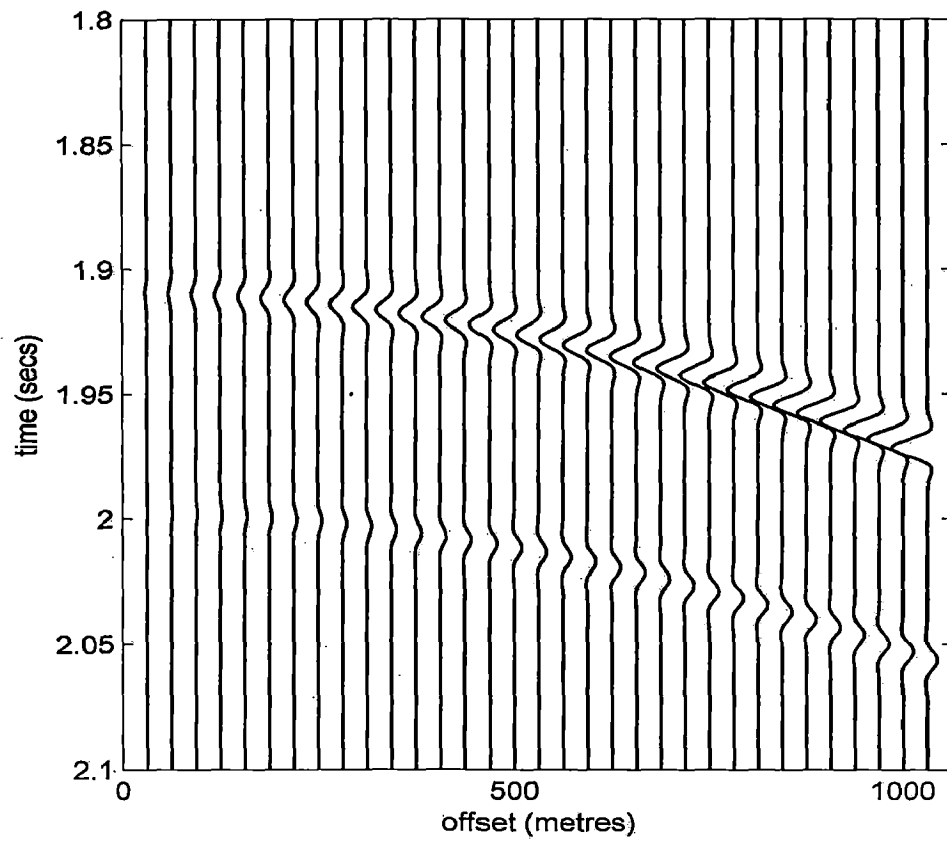Figure 4.7 : Synthetic Seismogram for model 2C   (A) – PP (B) - PS

36
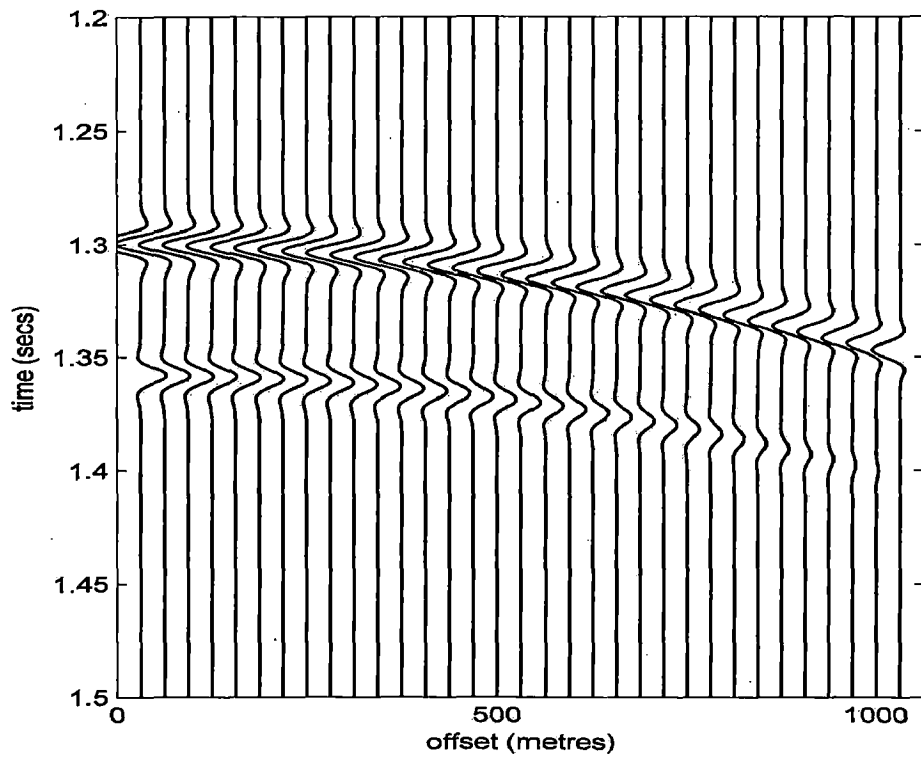
(A)

(B)

Figure 4.8 : Synthetic Seismogram for model 3A   (A) – PP (B) - PS

(A)

(B)

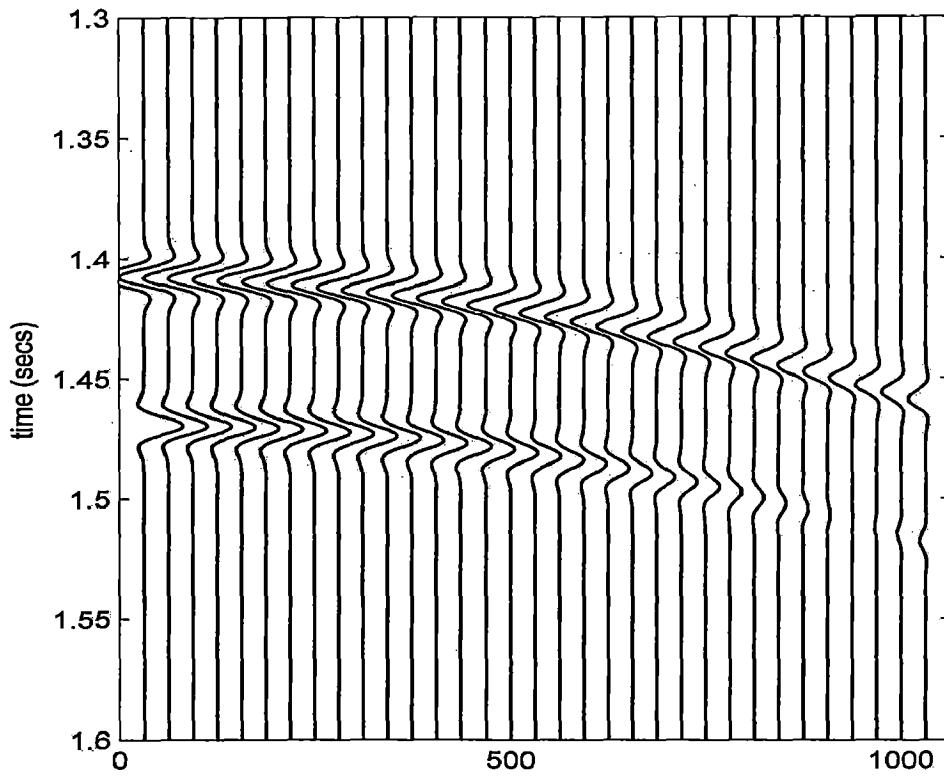Figure 4.9 : Synthetic Seismogram for model 3B   (A) – PP (B) - PS
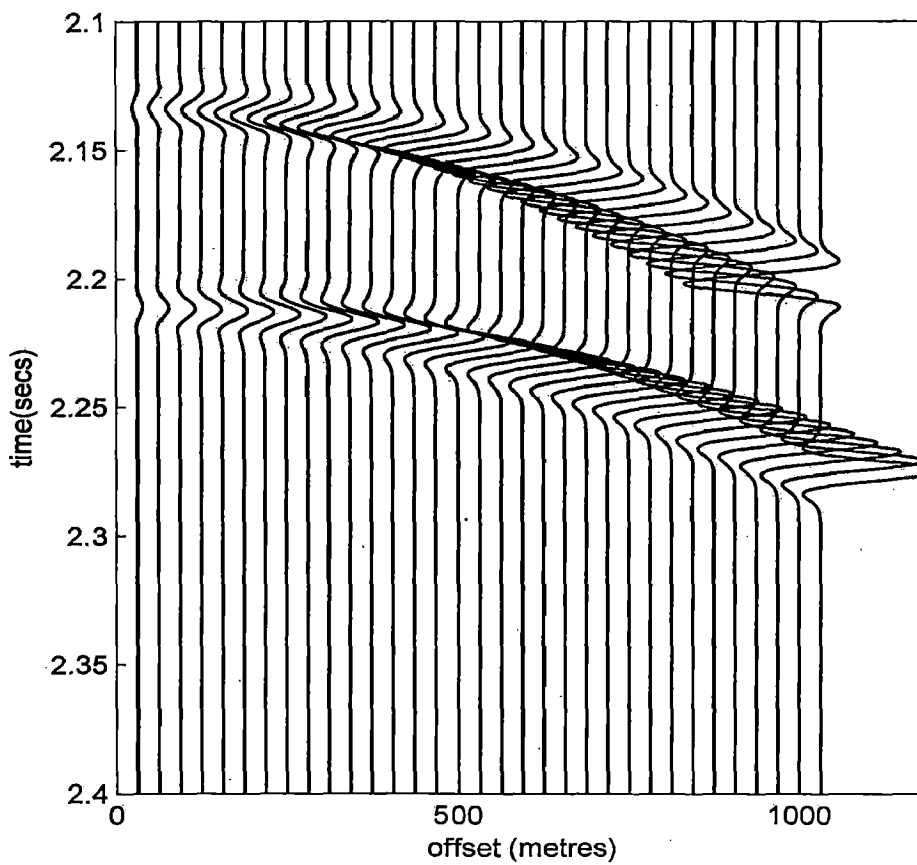
(A)

(B)

Figure 4.10 : Synthetic Seismogram for model 3C   (A) – PP (B) - PS
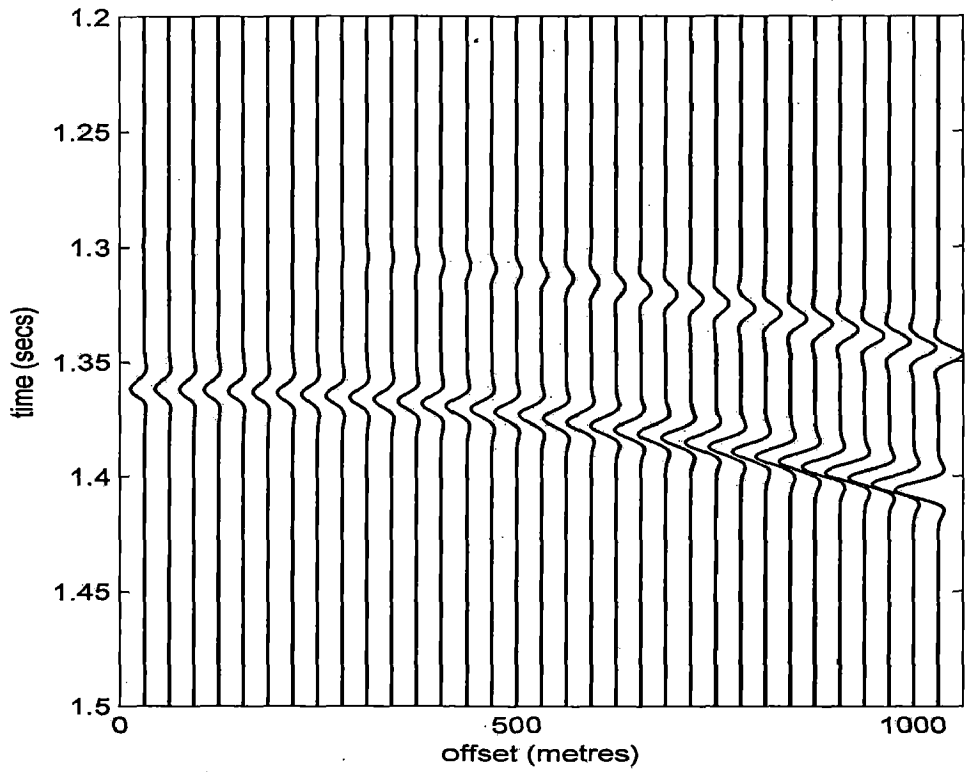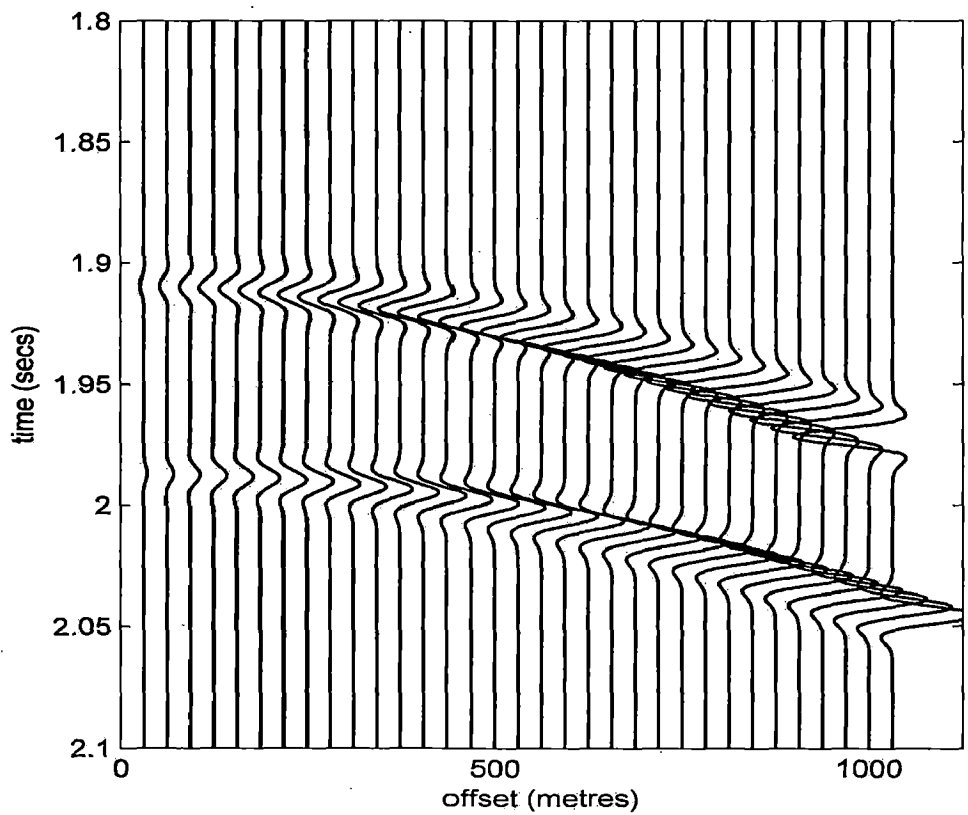
(A)

(B)

Figure 4.11 : Synthetic Seismogram for model 4A   (A) – PP (B) - PS
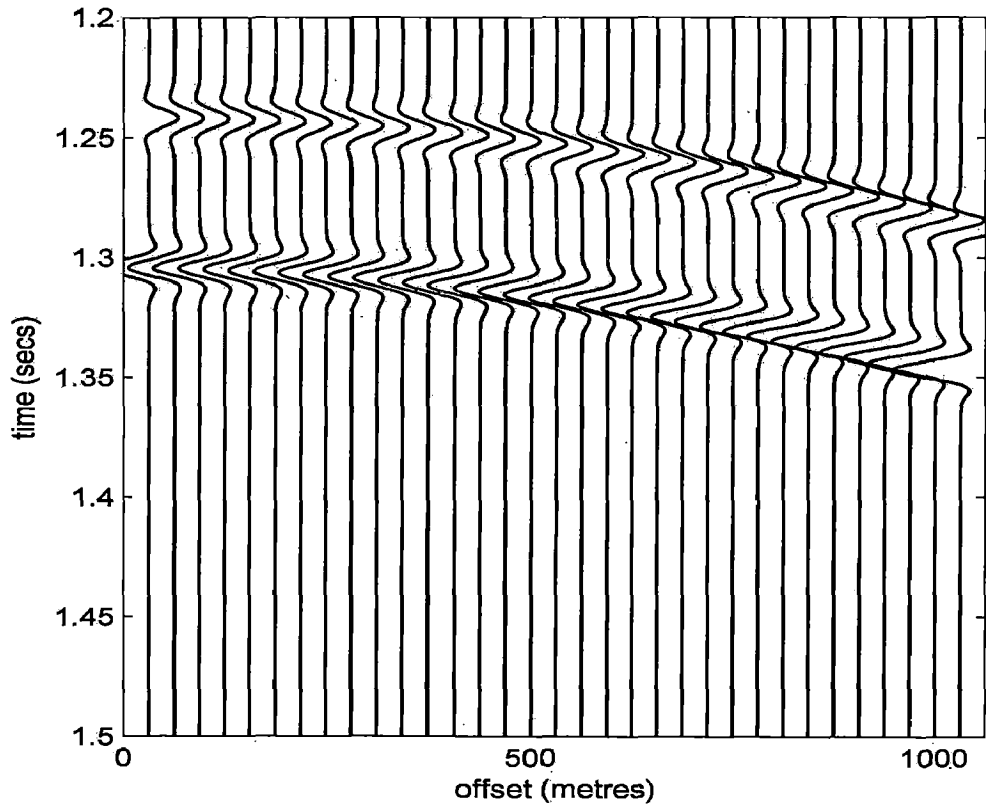
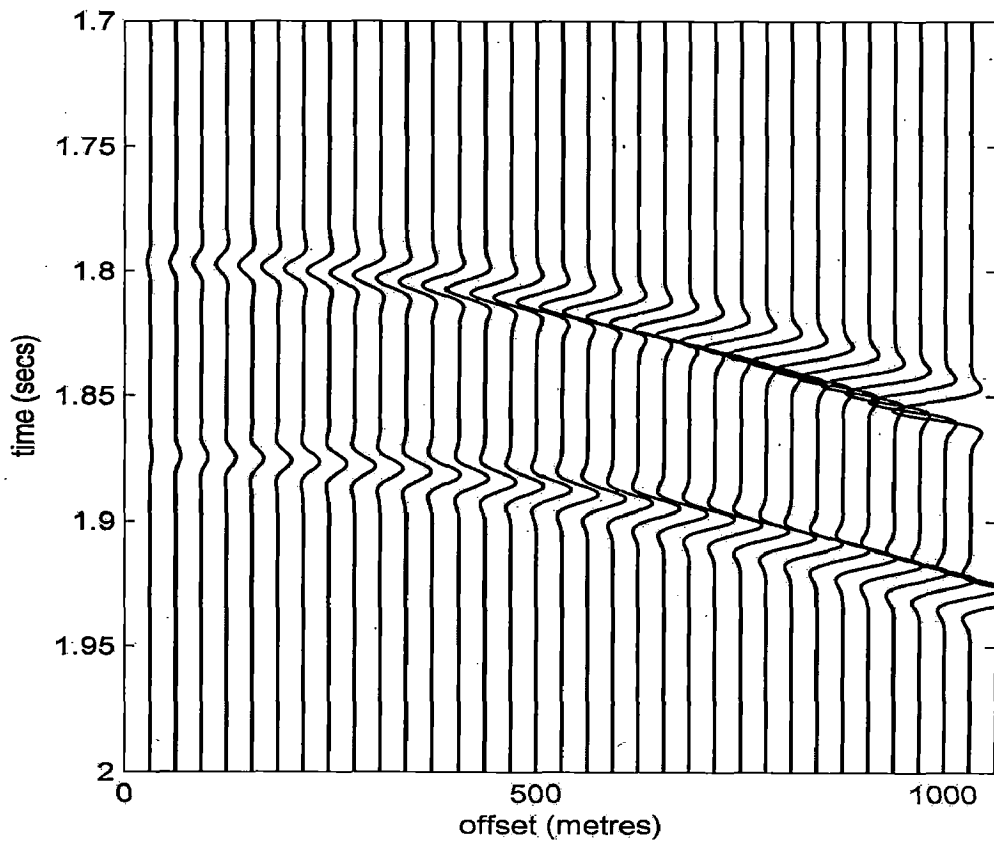(A)

(B)

Figure 4.12 : Synthetic Seismogram for model 4B   (A) – PP (B) - PS

(A)

(B)

Figure 4.13 : Synthetic Seismogram for model 4C   (A) – PP (B) - PS
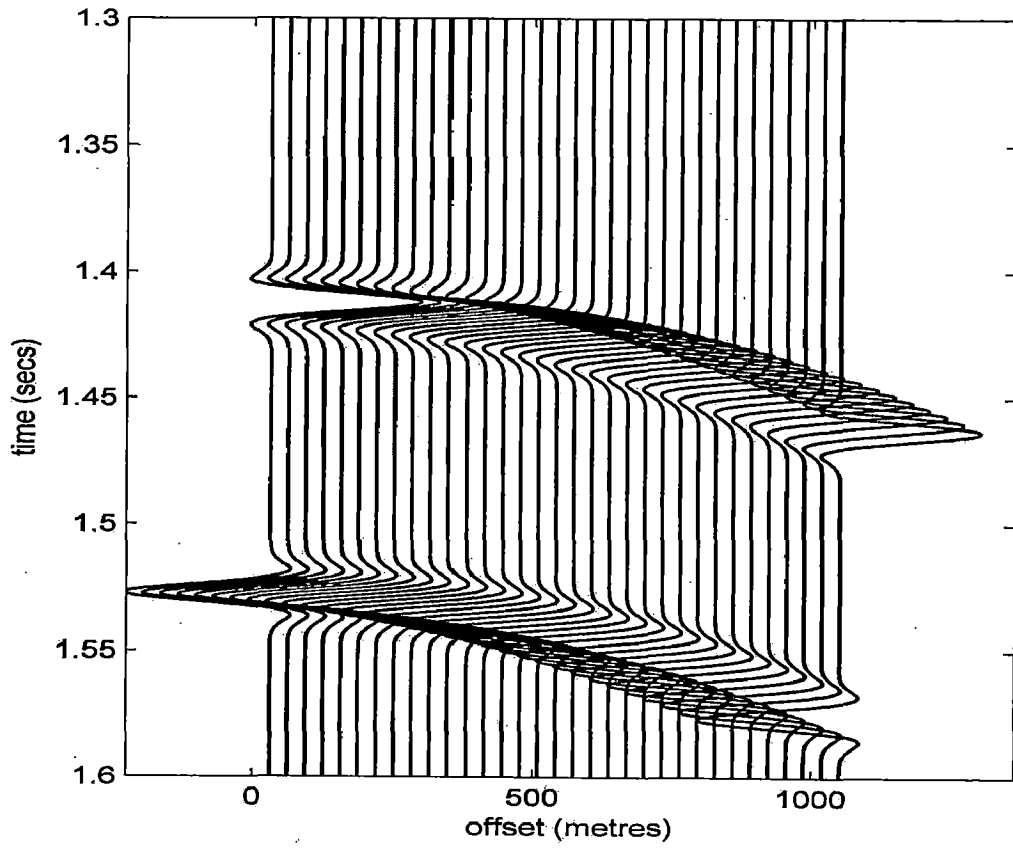
(A)
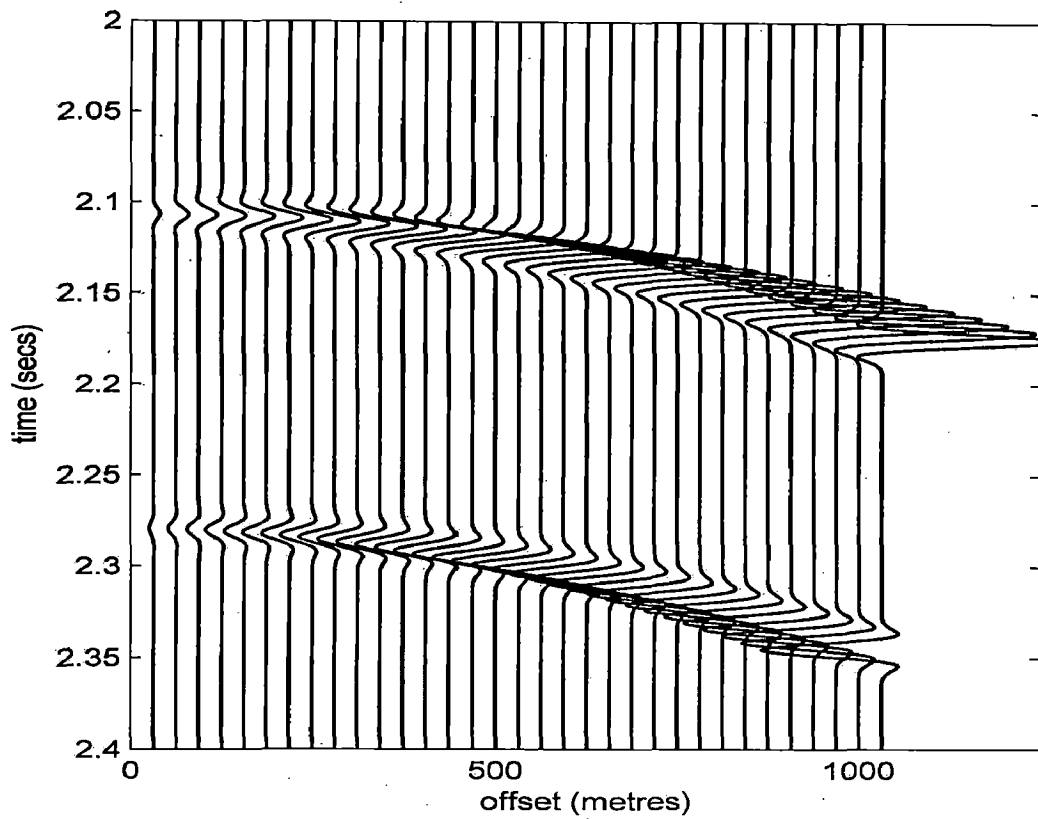
(B)

Figure 4.14 : Synthetic Seismogram for model 5   (A) – PP (B) - PS

Figure 4.15 (a): Relative % errors in P wave velocity for the first layer

Figure 4.15 (b): Relative % errors in P wave velocity for the second layer

Figure 4.16 (a): Relative % errors in density for the first layer

Figure 4.16 (b): Relative % errors in density for the second laye

Figure 4.17 (a): Relative % errors in S wave velocity for the first layer

Figure 4.17 (b): Relative % errors in S wave velocity for the second layer

CHAPTER 5

CONCLUSION

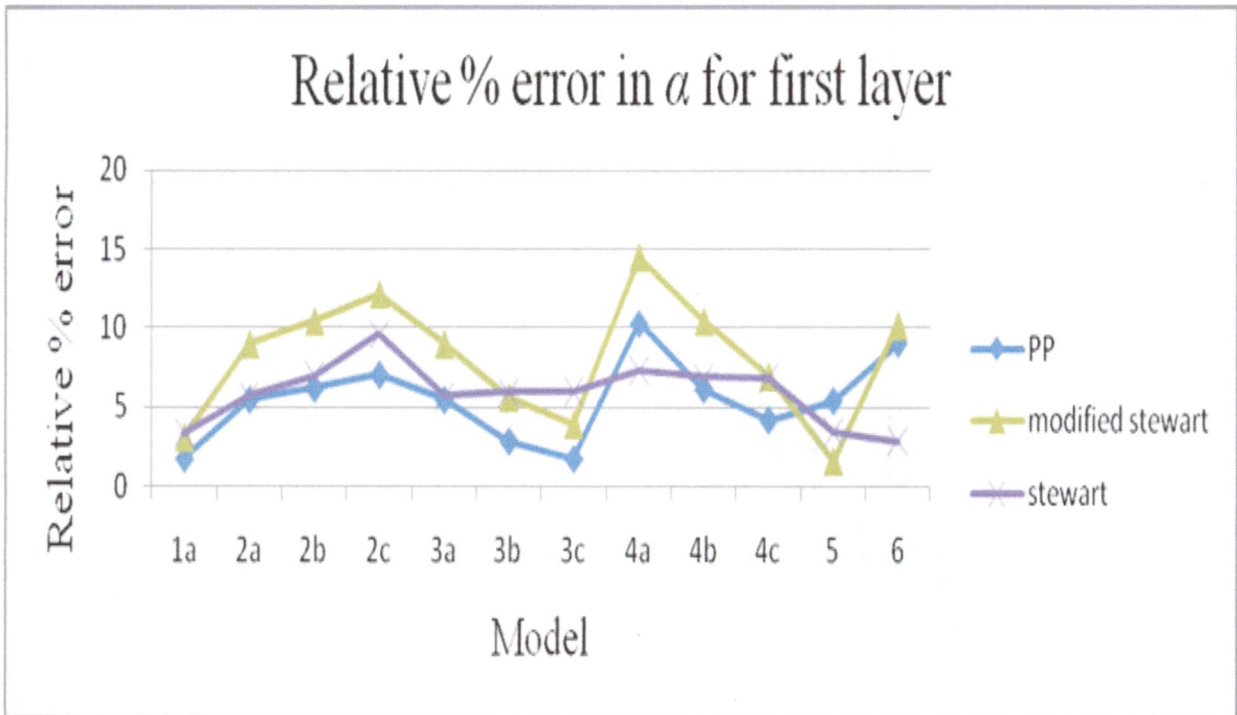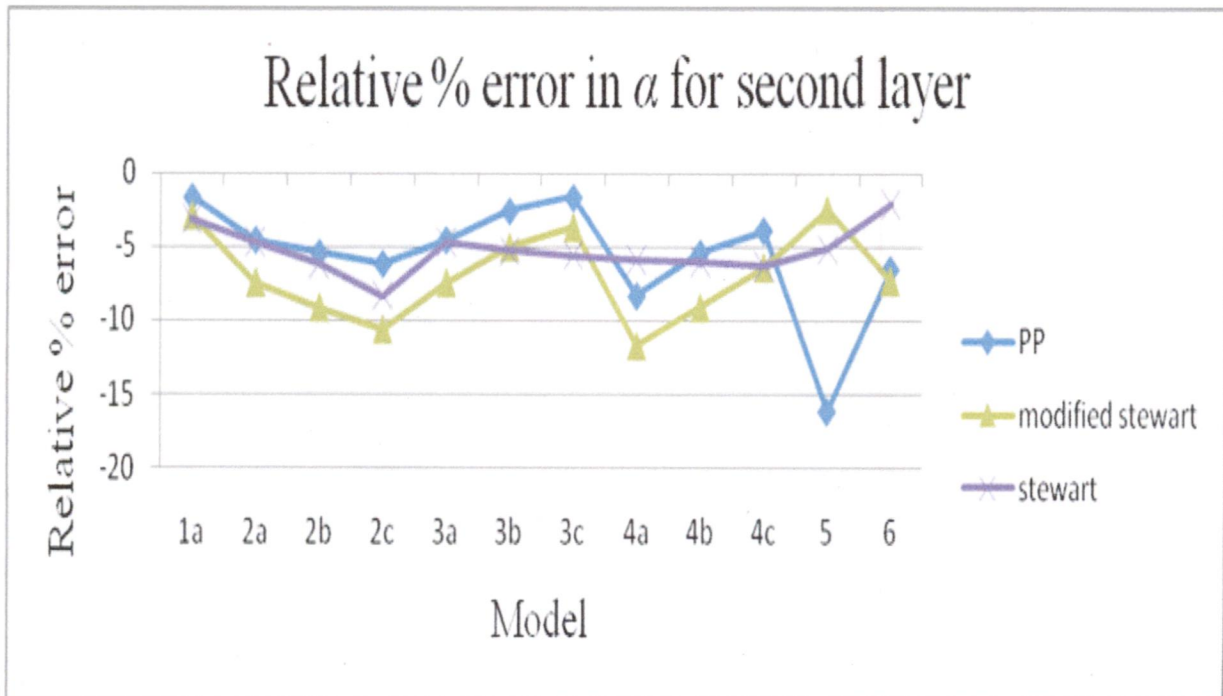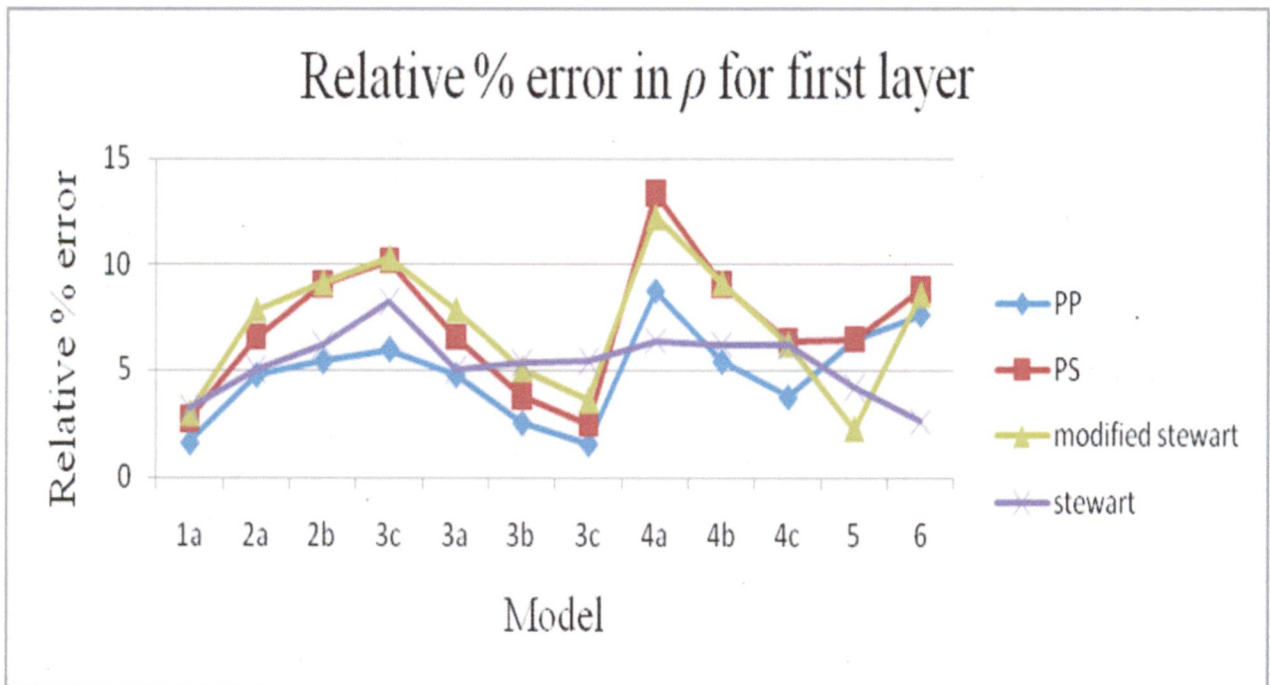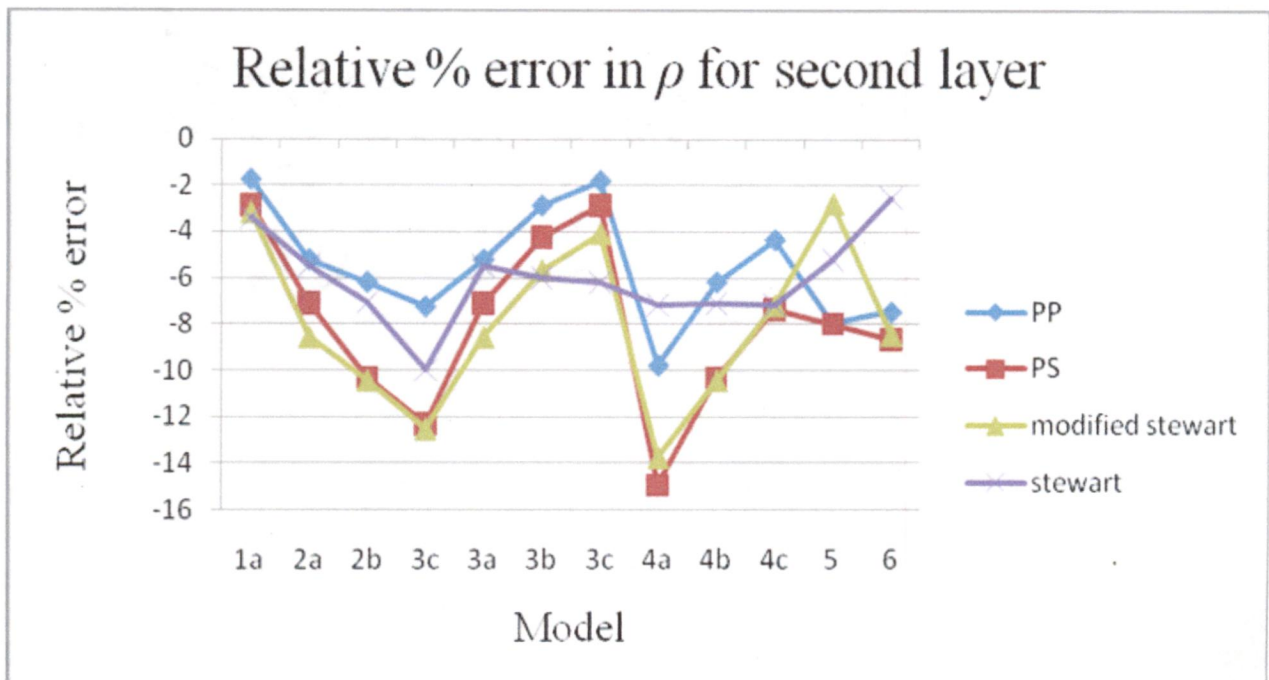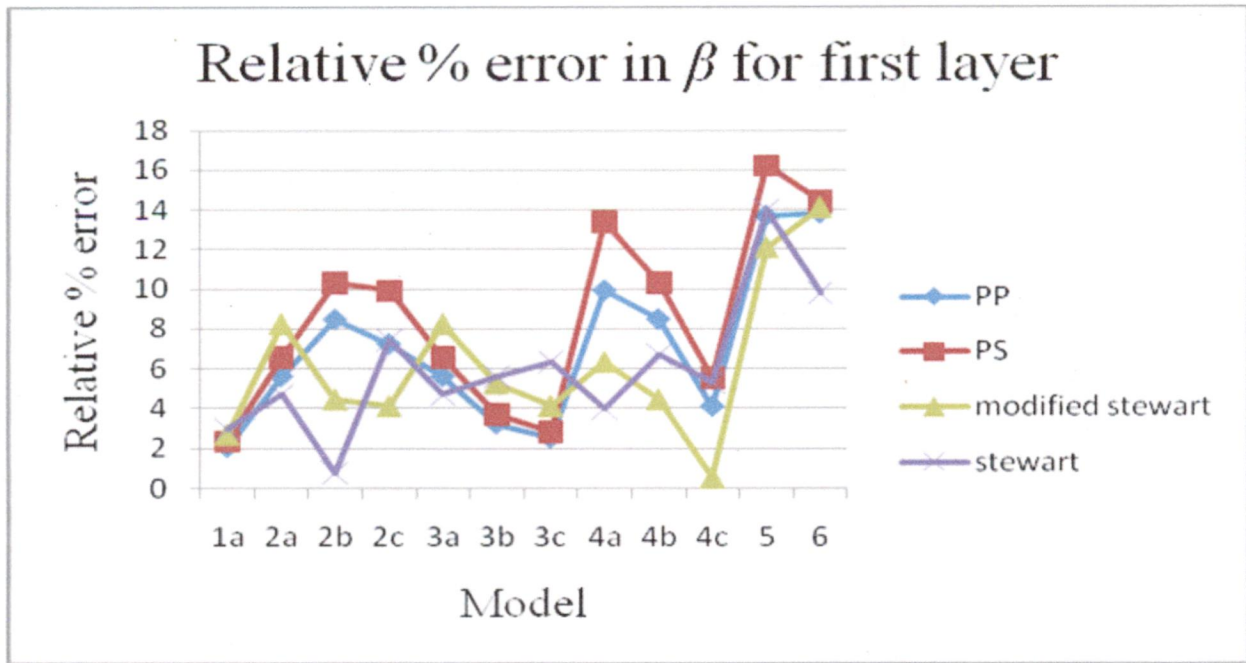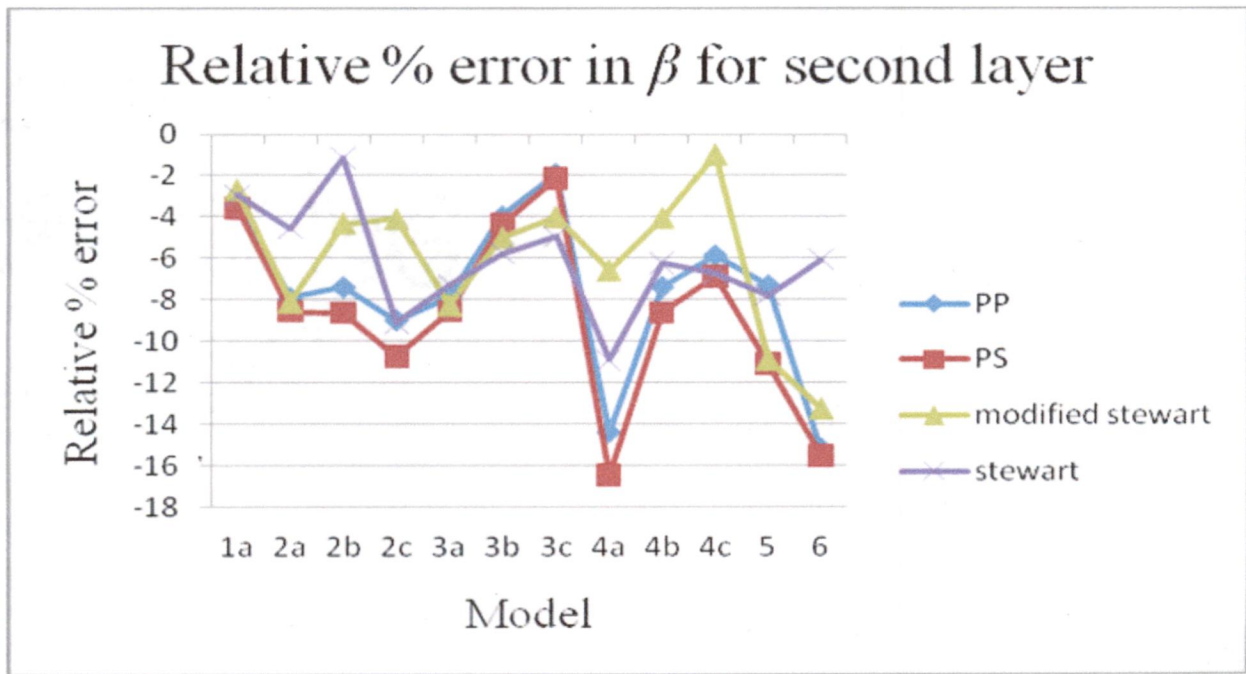In this study, the analysis of PP and PS AVO was conducted using several lithological models having different fluid contents. The study consisted of forward modelling and constructing synthetic seismograms for the models under consideration. Further ,the amplitude information contained in the first reflector in the synthetic data sets were inverted for the P wave velocity, S wave velocity and the density using three different inversion schemes. One of these schemes was based on the direct inversion using Aki Richards approximations, while the other two were based on a joint inversion methodology developed by Stewart (1990)

On the basis of the modelling and inversion studies carried out in the present work, the following conclusions have been arrived at:

1) Errors in the inverted values of the density, and P and S wave velocity are lower when the contrasts ($\Delta\rho/\rho, \Delta\alpha/\alpha$ and $\Delta\beta/\beta$) are low.

2) Errors in the PS inversion are higher than those in PP inversion using the Aki Richards approximation.

3) For lower contrasts, the PP data set is enough to invert for the values of α and ρ.

4) For significantly higher contrasts, joint inversion may provide better estimates of α and ρ.

5) For inverting for values of β, joint inversion is better as compared to using the PP and the PS datasets separately.

6) The two term joint inversion is in most cases better than the three term joint inversion (applicable to Stewart (1990)), except in case of higher contrasts.

7) The PS data set when used in conjunction with PP data set presents significant advantages in estimating the values of the model properties ρ, β and α and could be used for AVO analysis and interpretation.

REFERENCES

1. Aki, K., and Richards, P. G., 2002, Quantitative Seismology: Theory and Methods, University Science Books, Sausalito, California, pp. 700.

2. Castagna, J.P., 1993, Petrophysical Imaging using AVO, The Leading Edge, pp. 172-178.

3. Engelmark. F., 2001, Using 4C to Characterize Lithologies and Fluids in Clastic Reservoirs: The Leading Edge, 20, pp. 1053-1055.

4. Fatti, J.L., Smith, G.C., Vail, P.J., Strauss, P.J., and Levitt, P.R., 1994, Detection of gas in sandstone reservoirs using AVO analysis: Geophysics, 59, pp. 1362-1376.

5. Gardner, G. H. F., Gardner, L.W., and Gregory, A. R., 1974, Formation velocity and density: The diagnostic basis for stratigraphic traps: Geophysics, 39, pp. 770-780.

6. Ostrander, W. J., 1982, Plane wave reflection coefficients for gas sands at nonnormal angles of incidence: 52nd Annual Internat. Mtg., Soc. Expl. Geophys., Expanded Abstracts, 82, Session:S16.4.

7. Shuey, R.T., 1985, A simplification of the Zoeppritz equations, Geophysics 50, pp. 609-614.

8. Smith, G. C., and Gidlow, P. M., 1987, Weighted stacking for rock property estimation and detection of gas: Geophys. Prospec., 35, pp. 993-1014.

9. Stewart, R. R., 1990, Joint P and P-SV inversion: The CREWES Project Research Report, Vol. 2, pp. 112-115.

APPENDIX

A) Percentage relative errors for inversion in P wave velocity for the first two layers.

% relative errors in α for first layer				% relative errors in α for second layer			
Mode l	PP inversion	Modified Stewart inversion	Stewart inversion	Mode l	PP inversion	Modified Stewart inversion	Stewart inversion
1	1.743	3.138	3.382	1	-1.620	-2.915	-3.142
2A	5.461	8.957	5.695	2A	-4.528	-7.427	-4.722
2B	6.171	10.405	7.009	2B	-5.402	-9.109	-6.136
2C	7.041	12.139	9.563	2C	-6.136	-10.580	-8.334
3A	5.461	8.957	5.695	3A	-4.528	-7.427	-4.722
3B	2.858	5.626	5.939	3B	-2.549	-5.018	-5.298
3C	1.755	3.937	6.006	3C	-1.630	-3.658	-5.581
4A	10.282	14.465	7.326	4A	-8.299	-11.680	-5.913
4B	6.166	10.398	6.912	4B	-5.398	-9.103	-6.052
4C	4.217	6.963	6.866	4C	-3.866	-6.384	-6.294
5	5.427	1.646	3.455	5	-16.090	-2.455	-5.152
6	9.045	10.168	2.891	6	-6.493	-7.299	-2.075

B) Percentage relative errors for inversion in S wave velocity for the first two layers

\% relative errors in β and for first layer					\% relative errors in β for second layer				
Mo del	PP inversion	PS inversion	Modified Stewart inversion	Stewart inversion	Mo del	PP inversion	PS inversion	Modified Stewart inversion	Stewart inversioi
1	2.037	2.347	2.697	2.977	1	-3.350	-3.590	-2.699	-2.966
2A	5.602	6.557	8.240	4.699.	2A	-7.897	-8.553	-8.111	-4.544
2B	8.462	10.295	4.444	0.766	2B	-7.388	-8.619	-4.325	-1.134
2C	7.226	9.896	4.114	7.417	2C	-8.980	-10.718	-4.107	-9.105
3A	5.602	6.557	8.240	4.699	3A	-7.897	-8.553	-8.248	-7.277
3B	3.220	3.707	5.263	5.601	3B	-3.966	-4.333	-5.012	-5.764
3C	2.520.	2.822	4.126	6.358	3C	-1.903	-2.144	-4.009	-4.964
4A	9.917	13.386	6.335	3.987	4A	-14.395	-16.445	-6.584	-10.890
4B	8.466	10.295	4.444	6.716	4B	-7.377	-8.605	-4.057	-6.202
4C	4.087	5.521	0.518	5.324	4C	-5.849	-6.882	-1.000	-6.741
5	13.685	16.216	12.081	13.993	5	-7.298	-11.073	-10.876	-7.758
6	13.828	14.421	14.107	9.771	6	-15.194	-15.513	-13.246	-6.054

APPENDIX

C) Percentage relative errors for inversion in density for the first two layers

% relative errors in ρ for first layer					% relative errors in ρ for second layer				
Model	PP inversion	PS inversion	Modified Stewart inversion	Stewart inversion	Model	PP inversion	PS inversion	Modified Stewart inversion	Stewart inversion
1	1.627	2.698	2.971	3.199	1	-1.735	-2.876	-3.168	-3.410
2A	4.770	6.542	7.867	5.045	2A	-5.189	-7.118	-8.559	-5.489
2B	5.405	9.054	9.152	6.192	2B	-6.166	-10.329	-10.440	-7.064
2C	5.968	10.170	10.340	8.258	2C	-7.230	-12.32	-12.525	-10.003
3A	4.770	6.542	7.867	5.045	3A	-5.189	-7.118	-8.559	-5.489
3B	2.551	3.801	5.067	5.345	3B	-2.855	-4.253	-5.670	-5.981
3C	1.583	2.514	3.594	5.460	3C	-1.797	-2.854	-4.080	-6.199
4A	8.716	13.334	12.255	6.387	4A	-9.774	-14.952	-13.742	-7.162
4B	5.401	9.047	9.145	6.214	4B	-6.161	-10.32	-10.433	-7.088
4C	3.754	6.387	6.217	6.203	4C	-4.337	-7.379	-7.182	-7.167
5	6.436	6.454	2.253	4.208	5	-7.965	-7.988	-2.789	-5.208
6	7.603	8.820	8.604	2.608	6	-7.464	-8.659	-8.447	-2.561